1

Wireless Positioning: Fundamentals, Systems and State of the Art Signal Processing Techniques

Lingwen Zhang[1], Cheng Tao[1] and Gang Yang[2]
[1]*School of Electronics and Information Engineering, Beijing Jiaotong University*
[2]*School of Information Engineering, Communication University of China*
China

1. Introduction

With the astonishing growth of wireless technologies, the requirement of providing universal location services by wireless technologies is growing. The process of obtaining a terminal's location by exploiting wireless network infrastructure and utilizing wireless communication technologies is called wireless positioning (Rappaport, 1996). Location information can be used to enhance public safety and revolutionary products and services. In 1996, the U.S. federal communications commission (FCC) passed a mandate requiring wireless service providers to provide the location of a wireless 911 caller to the nearest public safety answering point (PSAP) (Zagami et al., 1998). The wireless E911 program is divided into two parts- Phase I and Phase II, carriers were required to report the phone number of the wireless E911 caller and the location (Reed, 1998). The accuracy demands of Phase II are rather stringent. Separate accuracy requirements were set forth for network-based and handset-based technologies: For network-based solution: within 100m for 67% of calls, and within 300m for 95% of the calls. For handset-based solutions: within 50m for 67% of calls and within 150m for 95% of calls. Now E911 is widely used in U.S. for providing national security, publish safety and personal emergency location service. Wireless positioning has also been found useful for other applications, such as mobility management, security, asset tracking, intelligent transportation system, radio resource management, etc. As far as the mobile industry is concerned, location based service (LBS) is of utmost importance as it is the key feature that differentiates a mobile device from traditional fixed devices (Vaughan-Nichols, 2009). With this in mind, telecommunications, devices, and software companies throughout the world have invested large amounts of money in developing technologies and acquiring businesses that would let them provide LBS. Numerous companies-such as Garmin, Magellan, and TomTom international-sell dedicated GPS devices, principally for navigation. Several manufactures-including Nokia and Research in Motion-sell mobile phones that provide LBS. Google's My Location service for mobile devices, currently in beta, uses the company's database of cell tower positions to triangulate locations and helps point out the current location on Google map. Various chip makers manufacture processors that provide devices with LBS functionality. These companies' products and services work together to provide location-based services, as Fig. 1. Shows (Vaughan-Nichols, 2009).

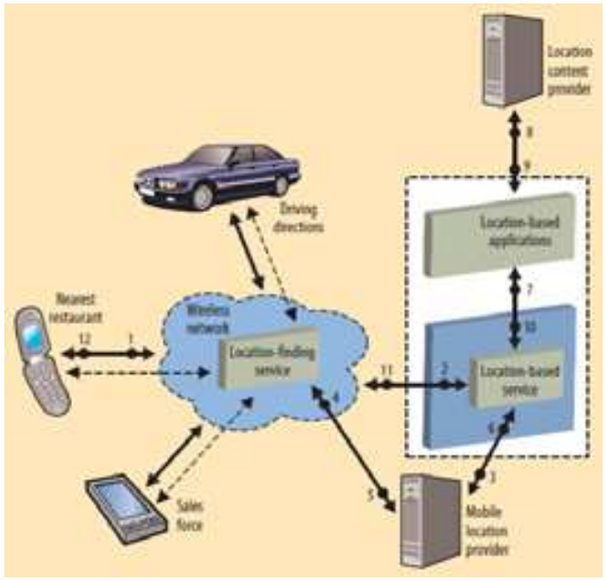

Fig. 1. Diagram shows how various products and services work together to provide location-based services

Thus, location information is extremely important. In order to help the growth of this emerging industry, there is a requirement to develop a scientific framework to lay a foundation for design and performance evaluation of such systems.

1.1 Elements of wireless positioning systems

Fig. 2. illustrates the functional block diagram of a wireless positioning system (Pahlavan, 2002). The main elements of the system are a number of location sensing devices that measure metrics related to the relative position of a mobile terminal (MT) with respect to a known reference point (RP), a positioning algorithm that processes metrics reported by location sensing elements to estimate the location coordinates of MT, and a position computing system that calculate the location coordinates. The location metrics may indicate the approximate arrival direction of the signal or the approximate distance between the MT and RP. The angle of arrival (AOA)/Direction finding (DF) is the common metric used in direction-based systems. The received signal strength (RSS), carrier signal phase of arrival (POA) and time of arrival (TOA), time difference of arrival (TDOA), frequency difference of arrival (FDOA)/Doppler difference (DD) of the received signal are the metrics used for estimation of distance. Which metrics should be measured depends on the positioning

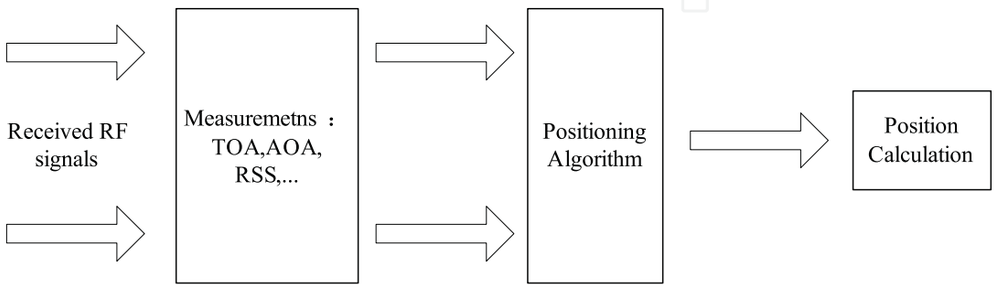

Fig. 2. Basic elements of a wireless positioning system

algorithms. As the measurements of metrics become less reliable, the complexity of the position calculation increased. Some positioning system also has a display system. The display system can simply show the coordinates of the MT or it may identify the relative location of the MT in the layout of an area. This display system could be software residing in a private PC or a mobile locating unit, locally accessible software in a local area network, or a universally accessible service on the web.

1.2 Location measuring techniques

As discussed in section 1.1, received signal strength (RSS), angle of arrival (AOA), time of arrival (TOA), round trip time (RTT), time difference of arrival (TDOA), phase of arrival (POA), and phase difference of arrival (PDOA) can all be used as location measurements (Zhao, 2006).

1.2.1 RSS estimation

RSS is based on predicting the average received signal strength at a given distance from the transmitter (Jian, 2005). Then, the measured RSS can provide ranging information by estimating the distance from the large-scale propagation model. Large-scale propagation model is used to estimate the mean signal strength for an arbitrary transmitter-receiver (T-R) separation distance since they characterize signal strength over large T-R separation distances (several hundreds or thousands of meters). The average large-scale propagation model is expressed as a function of distance by using a path loss exponent, n

$$P_r(d)[dBm] = P_r(d_0)[dBm] - 10n\log(\frac{d}{d_0}) + X_\sigma \tag{1}$$

Where $P_r(d)[dBm]$ is the received power in dBm units which is a function of the T-R distance of d, n is the path loss exponent which indicates the rate at which the path loss increased with distance, d is the T-R separation distance, d_0 is the close-in reference distance, as a known received power reference point. $P_r(d_0)[dBm]$ is the received power at the close-in reference distance. The value $P_r(d_0)[dBm]$ may be predicted or may be measured in the radio environment by the transmitter. For practical system using low-gain antennas in the 1-2GHz region, d_0 is typically chosen to be 1m in indoor environments and 100m or 1km in outdoor environments. X_σ describes the random shadowing effects, and is a zero-mean Gaussian distributed random variable (in dB) with standard deviation σ (also in dB). By measuring $P_r(d)[dBm]$ and $P_r(d_0)[dBm]$, the T-R distance of d may be estimated.
RSS measurement is comparatively simple for analysis and implementation but very sensitive to interference caused by fast multipath fading. The Cramer-Rao lower bound (CRLB) for a distance estimate provides the following inequality (Gezici, 2005):

$$\sqrt{Var(\hat{d})} \geq \frac{\ln 10}{10}\frac{\sigma}{n}d \tag{2}$$

Where d is the distance between the T-R, n is the path loss factor, and σ is the standard deviation of the zero mean Gaussian random variable representing the log-normal channel shadowing effect. It is observed that the best achievable limit depends on the channel parameters and the distance between the transmitter and receiver. It is suitable to use RSS measurements when the target node can be very close to the reference nodes.

1.2.2 TOA and TDOA estimation

TOA can be used to measure distance based on an estimate of signal propagation delay between a transmitter and a receiver since radiowaves travel at the speed of light in free space or air (Alavi,2006). The TOA can be measured by either measuring the phase of received narrowband carrier signal or directly measuring the arrival time of a wideband narrow pulse (Pahlavan, 2002). The ranging techniques of TOA measurement can be classified in three classes: narrowband, wideband and ultra wide band (UWB).

In the narrowband ranging technique, the phase difference between received and transmitted carrier signals is used to measure the distance. The phase of a received carrier signal, ϕ , and the TOA of the signal, τ ,are related by $\tau = \phi / \omega_c$,where ω_c is the carrier frequency in radio propagation. However, when a narrowband carrier signal is transmitted in a multipath environment, the composite received carrier signal is the sum of a number of carriers, arriving along different paths, of the same frequency but different amplitude and phase. The frequency of the composite received signal remains unchanged, but the phase will be different form one-path signal. Therefore, using a narrowband carrier signal cannot provide accurate estimate of distance in a heavy multipath environment.

The direct-sequence spread-spectrum (DSSS) wideband signal has been used in ranging systems. In such a system, a signal coded by a known pseudo-noise (PN) sequence is transmitted by a transmitter. Then a receiver cross correlates received signal with a locally generated PN sequence using a sliding correlator or a matched filter. The distance between the transmitter and receiver is determined from the arrival time of the first correlation peak. Because of the processing gain of the correlation process at the receiver, the DSSS ranging systems perform much better than other systems in suppressing interference.

Due to the scarcity of the available bandwidth in practice, the DSSS ranging systems cannot provide adequate accuracy. Inspired by high-resolution spectrum estimation techniques, a number of super-resolution techniques have been studied such as multiple signal classification (MUSIC) (Rieken, 2004).

For a single path additive white Gaussian noise (AWGN) channel, it can be shown that the best achievable accuracy of a distance estimate derived from TOA estimation satisfies the following inequality (Anouar, 2007):

$$\sqrt{Var(\hat{d})} \geq \frac{c}{2\sqrt{2}\pi\sqrt{SNR}\beta} \tag{3}$$

Where c is the speed of light, SNR is the signal-to-noise ratio, and β is the effective signal bandwidth defined by

$$\beta = [\int_{-\infty}^{\infty} f^2 \left|S(f)\right|^2 df \; / \int_{-\infty}^{\infty} \left|s(f)\right|^2 df]^{1/2}$$

and S(*f*) is the Fourier transform of the transmitted signal.

It is observed that the accuracy of a time-based approach can be improved by increasing the SNR or the effective signal bandwidth. Since UWB signals have very large bandwidths exceeding 500MHz, this property allows extremely accurate location estimates using time-based techniques via UWB radios. For example, with a receive UWB pulse of 1.5 GHz bandwidth, an accuracy of less than an inch can be obtained at SNR=0dB.

In general, direct TOA results in two problems. First, TOA requires that all transmitters and receivers in the system have precisely synchronized clocks (e.g.,just 1us of timing error

could result in a 300m position location error). Second, the transmitting signal must be labeled with a timestamp in order for the receiver to discern the distance the signal has traveled. For this reason, TDOA measurements are a more practical means of position location for commercial systems. The idea of TDOA is to determine the relative position of the mobile transmitter by examining the difference in time at which the signal arrives at multiple measuring units, rather than the absolute arrival time. Fig.3. is a simulation of a pulse waveform recorded by receivers P0 and P1. The red curve in Fig.3. is the cross correlation function. The cross correlation function slides one curve in time across the other and returns a peak value when the curve shapes match. The peak at time=5 is the TDOA measure of the time shift between the recorded waveforms.

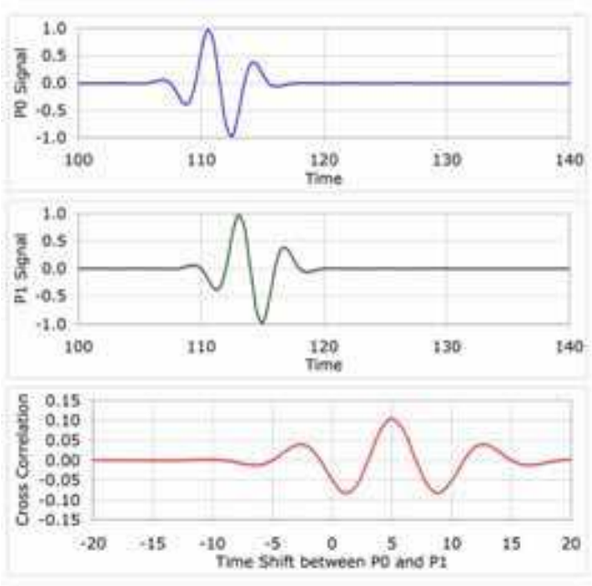

Fig. 3. Cross correlation method for TDOA measurements

1.2.3 AOA estimation

AOA is the measurement of signal direction through the use of antenna arrays. AOA metric has long and widely been studied in many years, especially in radar and sonar technologies for military applications. Using complicated antenna array, high-resolution angle measurement would be obtained.

The advantages of AOA are that a position estimate may be determined with as few as three measuring units for 3-D positioning or two measuring units for 2-D positioning, and that no time synchronization between measuring units is required. The disadvantages include relatively large and complex hardware requirements and location estimate degradation as the mobile target moves farther from the measuring units. For accurate positioning, the angle measurements need to be accurate, but the high accuracy measurements in wireless networks may be limited by shadowing, by multipath reflections arriving from misleading directions, or by the directivity of the measuring aperture. Some literatures also call AOA as direction of arrival (DOA) or direct finding (DF). Classic approaches for AOA estimation include Capon's method (Gershman, 2003; Stoica, 2003). The most popular AOA estimation techniques are based on the signal subspace approach by Schmidt (Swindlehurst, 1992) with

Multiple Signal Classification (MUSIC) algorithm. Subspace algorithms operate by separating a signal subspace from a noise subspace and exploiting the statistical properties of each. Variants of the MUSIC algorithm have been developed to improve its resolution and decrease its computational complexity including Root-MUSIC (Barabell, 1983) and Cyclic MUSIC. Other improved subspace-based AOA estimation techniques include the Estimation of Signal Parameters by Rotational Invariance Techniques (ESPRIT) algorithm and its variants, and a minimum-norm approach.

1.2.4 Joint parameter estimation

Estimators which estimate more than one type of location parameter (e.g., joint AOA/TOA) simultaneously have been developed. These are useful for hybrid location estimation schemes. Most joint estimators are based on ML techniques and signal subspace approaches, such as MUSIC or ESPRIT, and are developed for joint AOA/TOA estimation of a single users multipath signal components at a receiver.

The ML approach in (Wax & Leshem, 1997) for joint AOA/TOA estimation in static channels presents an iterative scheme that transforms a multidimensional ML criterion into two sets of one dimensional problems. Both a deterministic and a stochastic ML algorithm were developed in (Raleigh & Boros, 1998) for joint AOA/TOA estimation in time-varying channels. A novel subspace approach was proposed in (Vanderveen, Papadias & Paulraj, 1997) that jointly estimates the delays and AOAs of multipaths using a collection of space time channel estimates that have constant parameters of interest but different path fade amplitudes. Unlike MUSIC and ESPRIT, this technique has been shown to work when the number of paths exceeds that number of antennas.

1.3 Positioning algorithms

Once the location sensing parameters are estimated using the methods discussed in the previous section, it needs to be considered how to use these measurements to get the required position coordinates. In another words, how to design a geolocation algorithm with these parameters as input and position coordinates as output. In this section, the common methods for determining MT location will be described. It is to be noted that these algorithms assume measurements are made under Line of sight (LOS) conditions.

1.3.1 Geometric location

Geometric location uses the geometric properties to estimate the target location. It has three derivations: trilateration, multilateration and triangulation. Trilateration estimates the position of an object by measuring its distance from multiple reference points. Multilateration locates the object by computing the TDOA from that object to three or more receivers. Triangulation locates an object by computing angles relative to multiple reference points.

A. Trilateration

Trilateration is based on the measurement of distance (i.e. ranges) between MT and RP. The MT lies on the circumference of a circle, with the RP as center and a radius equal to the distance estimate. The desired MT location is determined by the intersection of at least three circle formed by multiple measurements between the MT and several RPs. Common methods for deriving the range measurements include TOA estimation and RSS estimation.

The solution is found by formulating the equations for the three sphere surface and then solving the three equations for the two unknowns: x and y, as shown in Fig.5. It is assumed that the MT located at (x,y), transmits a signal at time t_0, the three RPs located at $(x_1,y_1),(x_2,y_2),(x_3,y_3)$ receive the signal at time t_1,t_2,t_3. The equations for the three spheres are:

$$\sqrt{(x_i-x)^2+(y_i-y)^2}=c(t_i-t_0), i=1,2,3 \tag{4}$$

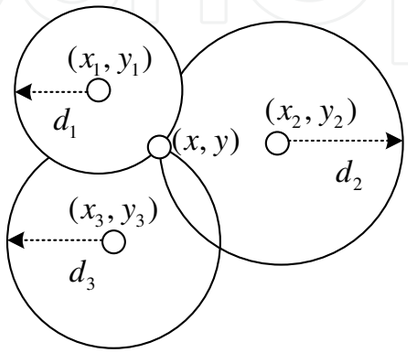

Fig. 5. Trilateration positioning

The next work to do is to find an optimized method to solve these equations under small error conditions. One well-known method is based on cost function. The cost function can be formed by

$$F(x)=\sum_{i=1}^{3}\alpha_i^2 f_i^2(x) \tag{5}$$

Where α_i can be chosen to reflect the reliability of the signal received at the measuring unit *i*, and $f_i(x)$ is given as follows.

$$f_i(x)=c(t_i-t_0)-\sqrt{(x_i-x)^2+(y_i-y)^2} \tag{6}$$

The location estimate is determined by minimizing the function $F(x)$. There are other algorithms such as closest-neighbor (CN) and residual weighting (RWGH). The CN algorithm estimates the location of the user as the location of the base station or reference point that is located closest to that user. The RWGH algorithm can be viewed as a form of weighted least-square algorithm.

B. Multilateration

Multilateration, also known as hyperbolic positioning, measures the time difference of signals travelled from a MT to a pair of RPs, or vice versa. The MT lies on a hyperbola defined by constant distance difference to the two RPs with the foci at the RPs. The desired location of the MT is determined at the intersection of the hyperbolas produced by multiple measurements as shown in Fig.6. This method requires no timestamp and only the synchronization among the RPs is required.

When the TDOA is measured, a set of equations can be described as follows.

$$R_{i,1} = c(t_i - t_1) = c\Delta\tau_i = R_i - R_1 \tag{7}$$

Where $R_{i,1}$ is the value of range difference from MT to the *i*th RP and the first RP.
Define

$$R_i = \sqrt{(X_i - x)^2 + (Y_i - y)^2}\ , \quad i = 1, \cdots N$$

(X_i, Y_i) is the RP coordinate, (x, y) is the MT location, R_i is the distance between the RP and MT, N is the number of BS, c is the light speed, $\Delta\tau_i$ is the TDOA between the service RP and the *i*th RP_i . In the geometric point of view, each equation presents a hyperbolic curve. Eq. (7) is a set of nonlinear equations. Fang (Fang, 1990) gave an exact solution when the number of equations is equal to the number of unknown coordinates. This solution, however, cannot make use of extra measurements, available when there are extra sensors, to improve position accuracy. In reality, the surfaces rarely intersect, because of various errors. In this case, the location problem can be posed as an optimization problem and solved using, for example, a least square method. The more general situation based on least square algorithm with extra measurements was considered by Friendlander (Friendlander, 1987). Although closed-form solution has been developed, the estimators are not optimum. Chen gave a closed-form, non-iterative solution utilizing the least square algorithm two times which performs well when the TDOA estimation errors are small. However, as the estimation errors increase, the performance declines quickly. Taylor-series method (Foy, 1976) is an iterative method which starts with an initial guess which is in the condition of close to the true solution to avoid local minima.

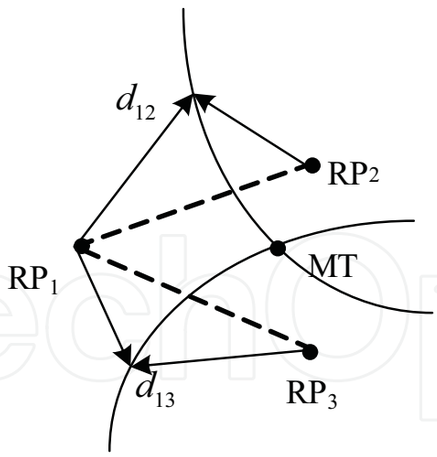

Fig. 6. Hyperbolic positioning

C. Triangulation positioning

When the AOA is measured, the location of the desired target can be found by the intersection of several pairs of angle direction lines. As shown in Fig. 7., at least two known RP and two measured angles are used to derive the 2-D location of the MT. The advantages of triangulation are that a position estimate may be determined with as few as three measuring units for 3-D positioning or two measuring units for 2-D positioning, and that no

time synchronization between measuring units is required. In cellular systems, the deployment of smart antenna makes AOA practical. However, the drawback of this method includes complexity and cost for the deployment of antennas at the RP side and impractical implementation at the MT side; susceptibility to linear orientation of RPs; accuracy deterioration with the increase in distance between the MT and the RP owing to fundamental limitations of the devices used to measure the arrival angles. The accuracy is limited by shadowing, multipath reflections arriving from misleading directions, or the directivity of the measuring aperture.

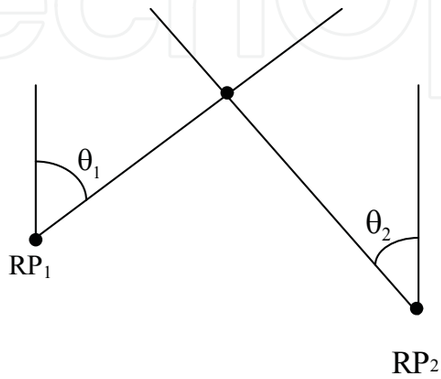

Fig. 7. Triangulation positioning

1.3.2 Hybrid positioning

Since the above reviewed location methods complement each other, hybrid techniques, which use a combination of available range, range-difference or angle measurements, or other methods to solve for locations, have been extensively investigated (see for example). Hybrid techniques are also studied to combat the problems, e.g. hearability (Zhao, 2006), accuracy , NLOS problems which will be discussed in the next section. Hybrid methods are especially useful in hearability conditions when the number of available BSs in cellular networks is limited. Most typical hybrid method combines TOA (TDOA) location with AOA location (Thomas, 2001). The scheme proposed in (Catovic & Sahinoglu, 2004) combines TDOA with RSS measurements.

1.3.3 Fingerprinting

Fingerprinting refers to techniques that match the fingerprint of some characteristic of a signal that is location dependent. There are two stages for location fingerprinting: offline stage and online stage. During the offline stage, a site survey is performed in an environment. The location coordinates and respective signal strengths from nearby RPs are collected. During the online stage, a fingerprinting algorithm is used to identify the most likely recorded fingerprinting to the measured one and to infer the target location. The main challenges to the techniques based on location fingerprinting is that the received signal strength could be affected by diffraction, reflection, and scattering in the propagation environments. There are at least five location fingerprinting-based positioning algorithm using pattern recognition technique so far: probabilistic methods, k-nearest-neighbor, neural networks, support vector machine, and smallest M-vertex polygon.

In urban areas, when the multipath problem is quite severe, both AOA and TOA/TDOA may encounter difficulties. To solve this problem, the multipath characteristics can be

considered as the fingerprinting of mobile phones, as shown in Fig. 8. The design involves a location server with a database that includes measured and predicted signal characteristics for a specific area. When an E911 call is made, the location of the mobile phone can be computed by comparing signals received by the mobile with the signal values stored in the database. Various signal characteristics, including received signal levels and time delays may be utilized.

Using a multipath delay profile to locate a mobile terminal is possible with fingerprinting. This avoids many of the problems that multipath propagation posed for conventional location methods. This method could obtain high accurate location as long as offline stage collects adequate and update information. However, the high cost for deployment and maintenance is obvious and unavoidable. As a result, it is a promising technique but not a mainstream option for the time being.

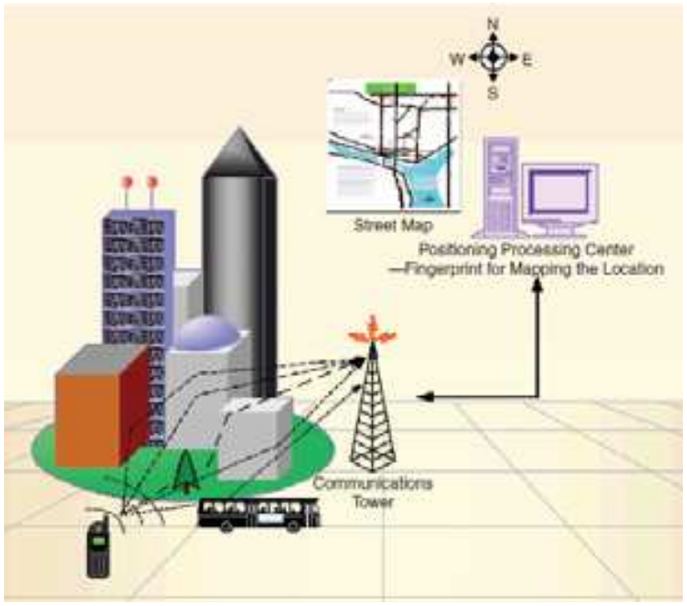

Fig. 8. Fingerprinting of mobile phones

2. Current location systems

Network-aided positioning has attracted much research attention in recent years. Different network topologies pose various technical challenges to design faster, more robust and more accurate positioning systems. There are numerous methods for obtaining the location information, depending on different location systems.

Location systems can be grouped in many different ways, including indoor versus outdoor systems or cellular versus sensor network positioning, as shown in Fig.9 (Guolin, 2005). Global positioning systems and cellular based location system can be used for outdoor positioning while indoor location used existing wireless local access network (WLAN) infrastructures for positioning. An overview of indoor positioning versus outdoor positioning by satellite is shown in Table 1. Sensor networks vary significantly from traditional cellular networks, where access nodes are assumed to be small, inexpensive, cooperative, homogeneous and often relatively autonomous. A number of location-aware

protocols have been proposed for "ad hoc" routing and networking. Sensor networks have also been widely used for intrusion detection in battlefields as well as for monitoring wildlife.

Different network topologies, physical layer characteristics, media access control layer characteristics, devices and environment require remarkably different positioning system solutions. In this section, an overview of positioning solutions applied in GPS, cellular networks and WLAN will be provided.

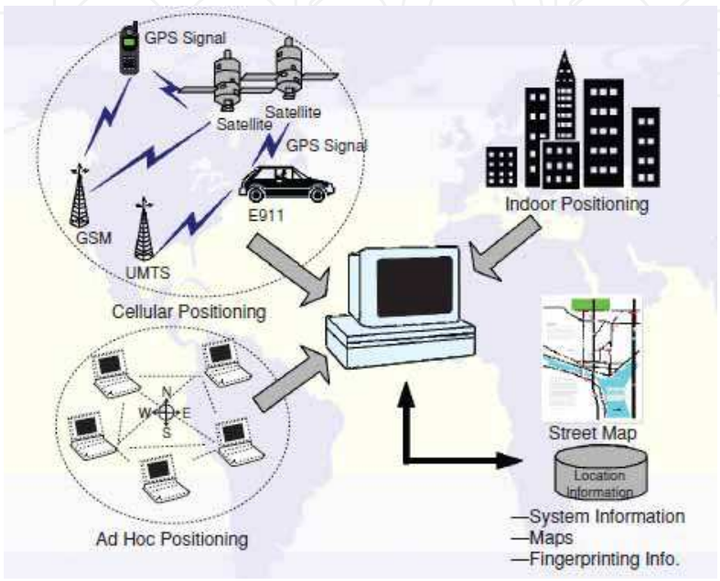

Fig. 9. Overview of indoor versus outdoor positioning systems

INDOOR	OUTDOOR (POSITIONING BY SATELLITE)
WLAN —CLIENT-BASED SYSTEM DESIGN —CLIENT-ASSISTED SYSTEM DESIGN	GPS —REQUIRES MINIMAL OBSTRUCTIONS —LONG ACQUISITION TIMES (30 s–15 min) —HAS TO BE SYNCHRONOUS —HIGH POWER CONSUMPTION AND HIGH UNIT COST
SENSOR NETWORK —LOCALIZATION WITH BEACONS —LOCALIZATION WITH MOVING BEACONS —BEACON-FREE LOCALIZATION	A-GPS —MUCH MORE ACCURATE: ACCURACY OF 10–50 m CAN BE USED EVEN FOR INDOOR POSITIONING —IMPROVES ACQUISITION TIME (< 10 s) —SYNCHRONOUS OR ASYNCHRONOUS —MORE COST EFFECTIVE THAN GPS —LITTLE/NO HARDWARE CHANGES REQUIRED IN BASE STATIONS
UWB —A PROMISING APPROACH FOR INDOOR GEOLOCATION —CAN ACHIEVE VERY ACCURATE SHORT DISTANCE ESTIMATION	

Table. 1. Overview of indoor positioning versus outdoor positioning by satellite

2.1 GPS

The Global Positioning System (GPS) is a satellite-based positioning system that can provide 3-D position and time information to users in all weather and at all times and anywhere on or near the earth when and where there is an unobstructed line of sight to four or more GPS satellites. It is maintained by the United States government and is freely accessible by anyone with a GPS receiver. GPS was created by U.S. Department of Defense and was originally run with 24 satellites. It was established in 1973.

2.1.1 GPS structure

GPS consists of three parts: the space segment, the control segment and the user segment. The space segment is composed of 24 to 32 satellites in medium earth orbit and also includes the boosters required to launch them into orbit. As of March 2008, there are 31 active broadcasting satellites in the GPS constellation shown in Fig.10., and two older, retired from active service satellites kept in the constellation as orbital spares. The additional satellites improve the precision of GPS receiver calculations by providing redundant measurements. The control segment is composed of a master control station, an alternate master control station, and a host of dedicated and shared ground antennas and monitor stations. The user segment is composed of hundreds of thousands of U.S. and allied military users of the secure GPS precise positioning service, and tens of millions of civil, commercial, and scientific users of the standard positioning service. In general, GPS receivers are composed of an antenna, receiver-processors and a highly stable clock.

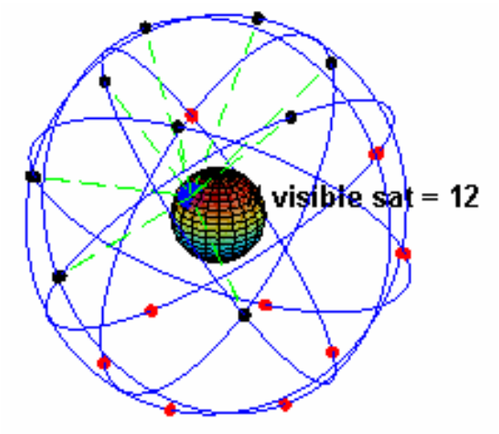

Fig. 10. GPS constellation

2.1.2 GPS signals

Each GPS satellite continuously broadcasts a navigation message at a rate of 50 bits per second. Each complete message is composed of 30 second frames shown in Fig. 11. All satellites broadcast at the same two frequencies, 1.57542GHz (L1 signal) and 1.2276 GHz (L2 signal). The satellite network uses a CDMA spread-spectrum technique where the low bit rate message data is encoded with a high rate pseudo random (PN) sequence that is different for each satellite as shown in Fig. 12. The receiver must be aware of the PN codes for each satellite to reconstruct the actual message data. The C/A code, for civilian use, transmits data at 1.023 million chips per second, whereas the P code, for U.S. military use, transmits at 10.23 million chips per second. The L1 carrier is modulated by both the C/A and P codes, while the L2 carrier is only modulated by the P code. The P code can be encrypted as a so-called P(Y) code which is only available to military equipment with a proper decryption key.

Since all of the satellite signals are modulated onto the same L1 carrier frequency, there is a need to separate the signals after demodulation. This is done by assigning each satellite a unique binary sequence known as a Gold code. The signals are decoded after demodulation, using addition of the Gold codes corresponding to the satellite monitored by the receiver as shown in Fig. 13.

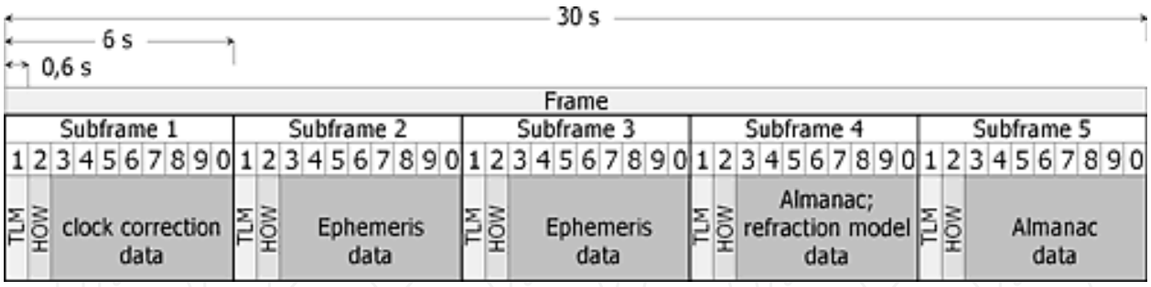

Fig. 11. GPS message frame

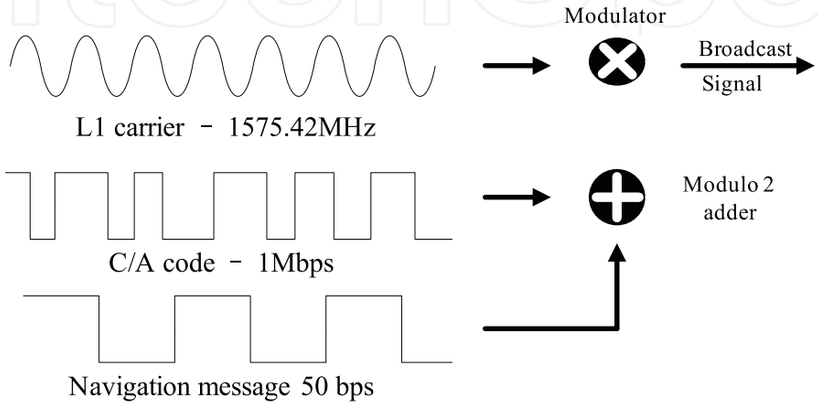

Fig. 12. Modulating and encoding GPS satellite signal using C/A code

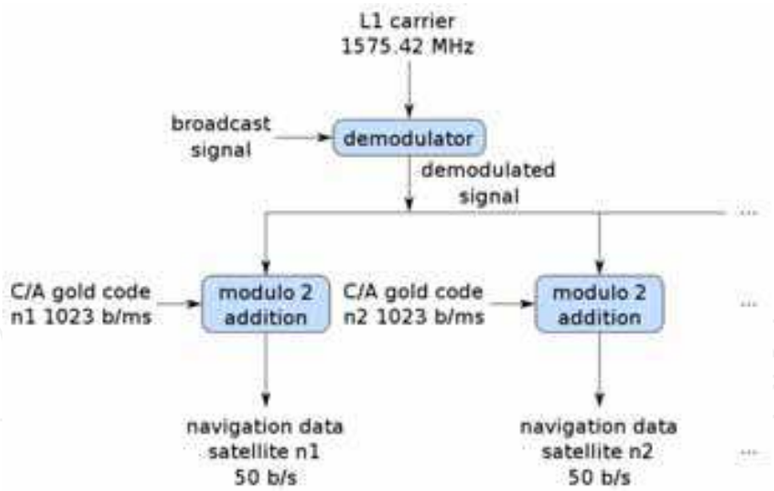

Fig. 13. Demodulating and decoding GPS satellite signal using C/A code

When the receiver uses messages to obtain the time of transmission and the satellite position, trilateration method is used to form equations and optimized algorithm is used to solve the equations as mentioned above.

The main advantages of GPS are its global coverage and high accuracy within 50 meters. And GPS receivers are not required to transmit anything to satellites, so there is no limit to the number of users that can use the system simultaneously. However, there also exist several issues that affect the effectiveness of GPS, especially in dealing with emergency

services: response time, the time to first fix (TTFF) which may be greater than 30 seconds. Besides, GPS cannot provide accurate location under the obstructed signal case (e.g. in the unban city area, inside buildings). Taking these drawbacks into consideration, GPS are not suitable for some location services such as emergency call.

2.2 Standardization methods for positioning in cellular networks

There are various location techniques that are used in cellular-based positioning system. They can be classified by three types: mobile-based solution in which the positioning is carried out in handset and sent back to the network, mobile-assisted solution in which handset makes the measurements, reports these to the network where the serving mobile location center node calculated the position, and network-based solution in which the measuring and positioning are done by network.

In 1997, TIA led the standardization activities for the positioning in GSM. Four positioning methods were included. They are cell identity and timing advance, uplink time of arrival, enhanced observed time difference (E-OTD) and Assisted GPS (A-GPS). There are two stages of standardizations, the first version specification supports circuit-switch connections and the second version specification provides the same support in the packet-switch domain.

Cell-ID is a simple positioning method based on knowing which cell sector the target belongs to. The sector is known only during an active voice or data call. With this method, no air interface resources are required to obtain cell sector information (if the user is active), and no modifications to handset hardware are required. The disadvantage obviously is that the location is roarse.

Time advance (TA) represents the round trip delay between the mobile and serving base station (BS), it is represented by a 6-bit integer number in the GSM frame. In addition, RXLEV is the measurement of the strength of signals received by a mobile, therefore, with suitable propagation models, the distance between a mobile and BS can be estimated.

Since Cell-ID is not accurate, Cell-ID+TA and Cell-ID+TA+RXLEV such hybrid positioning methods are used as shown in Fig.14.

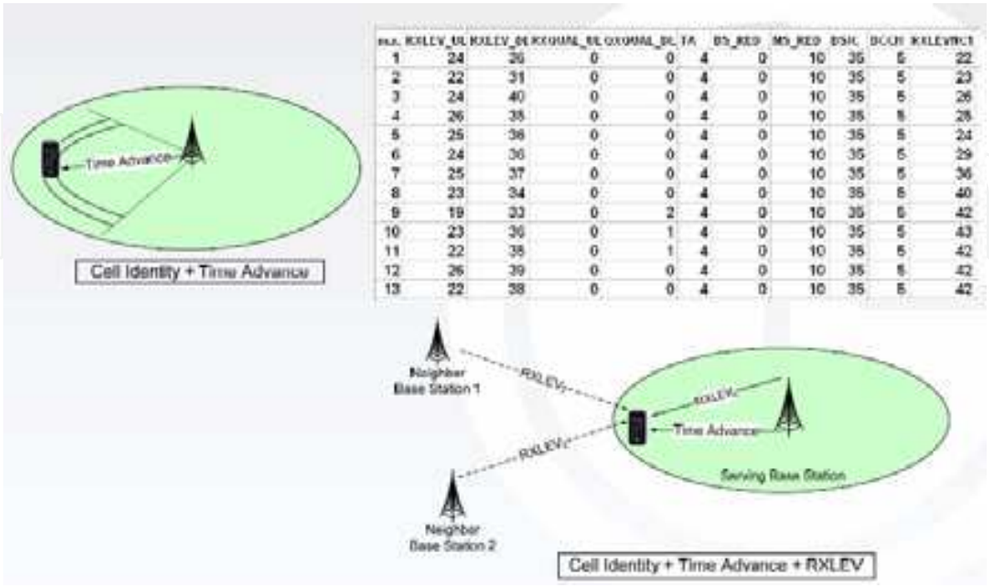

Fig. 14. Cell-ID with TA for GSM

E-OTD is based on TDOA measured by the mobile between the receptions of bursts transmitted from the reference BS and each neighboring BS which value is called geometric time difference (GTD), requiring a synchronous network. However, GSM is not synchronous. Location measurement unit (LMU) devices are therefore required to compute the synchronization difference between two BSs which is called real time difference (RTD). The GTD can be obtained by GTD=OTD-RTD. Fig. 15 illustrates the solution of E-ODT.

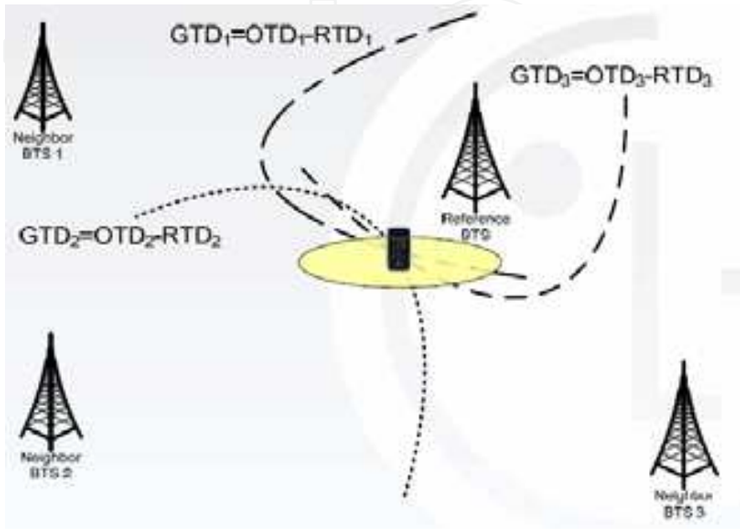

Fig. 15. E-OTD positioning for GSM

In the A-GPS for GSM, the GSM network informs the mobile about the data that GPS satellites are sending.

The standard positioning methods supported within UTRAN are:

- Cell-ID based method;
- OTDOA method that may be assisted by network configurable idle periods;
- Network-assisted GNSS methods;
- U-TDOA.

In the cell ID based (i.e. cell coverage) method, the position of an UE is estimated with the knowledge of its serving Node B. The information about the serving Node B and cell may be obtained by paging, locating area update, cell update, URA update, or routing area update. The cell coverage based positioning information can be indicated as the Cell Identity of the used cell, the Service Area Identity or as the geographical co-ordinates of a position related to the serving cell. The position information shall include a QoS estimate (e.g. regarding achieved accuracy) and, if available, the positioning method (or the list of the methods) used to obtain the position estimate. When geographical co-ordinates are used as the position information, the estimated position of the UE can be a fixed geographical position within the serving cell (e.g. position of the serving Node B), the geographical centre of the serving cell coverage area, or some other fixed position within the cell coverage area. The geographical position can also be obtained by combining information on the cell specific fixed geographical position with some other available information, such as the signal RTT in FDD or Rx Timing deviation measurement and knowledge of the UE timing advance, in TDD.

In OTDOA-IPDL method, the Node B may provide idle periods in the downlink, in order to potentially improve the hearability of neighbouring Node Bs. The support of these idle periods in the UE is optional. Support of idle periods in the UE means that its OTDOA

performance will improve when idle periods are available. Alternatively, the UE may perform the calculation of the position using measurements and assistance data.
Global Navigation Satellite System (GNSS) methods make use of UEs, which are equipped with radio receivers capable of receiving GNSS signals. Examples of GNSS include GPS, Modernized GPS, Galileo, GLONASS, Satellite Based Augmentation Systems (SBAS), and Quasi Zenith Satellite System (QZSS).In this concept, different GNSS (e.g. GPS, Galileo, etc.) can be used separately or in combination to perform the location of a UE.
The U-TDOA positioning method is based on network measurements of the Time of Arrival (TOA) of a known signal sent from the UE and received at four or more LMUs. The method requires LMUs in the geographic vicinity of the UE to be positioned to accurately measure the TOA of the bursts. Since the geographical coordinates of the measurement units are known, the UE position can be calculated via hyperbolic trilateration. This method will work with existing UE without any modification.
The standard positioning methods supported for E-UTRAN access are:
- network-assisted GNSS methods;
- downlink positioning;
- hanced cell ID method.

Hybrid positioning using multiple methods from the list of positioning methods above is also supported.
These positioning methods may be supported in UE-based, UE-assisted/E-SMLC-based, or eNB-assisted versions. Table 2 indicates which of these versions are supported in this version of the specification for the standardized positioning methods.

Method	**UE-based**	**UE-assisted, E-SMLC-based**	**eNB-assisted**	**SUPL**
A-GNSS	Yes	Yes	No	Yes (UE-based and UE-assisted
Downlink	No	Yes	No	Yes (UE-assisted)
E-CID	No	Yes	Yes	Yes (UE-assisted)

Table 2. Supported versions of UE positioning methods

The downlink (OTDOA) positioning method makes use of the measured timing of downlink signals received from multiple eNode Bs at the UE. The UE measures the timing of the received signals using assistance data received from the positioning server, and the resulting measurements are used to locate the UE in relation to the neighbouring eNode Bs.
Enhanced Cell ID (E-CID) positioning refers to techniques which use additional UE and/or E-UTRAN radio resource and other measurements to improve the UE location estimate. Although E-CID positioning may utilize some of the same measurements as the measurement control system in the RRC protocol, the UE generally is not expected to make additional measurements for the sole purpose of positioning; i.e., the positioning procedures do not supply a measurement configuration or measurement control message, and the UE reports the measurements that it has available rather than being required to take additional measurement actions. In cases with a requirement for close time coupling between UE and eNode B measurements (e.g., TADV type 1 and UE Tx-Rx time difference), the eNode B

configures the appropriate RRC measurements and is responsible for maintaining the required coupling between the measurements.

2.3 Indoor location system

Since cellular-based positioning methods or GPS cannot provide accurate indoor geolocation, which has its own independent applications and unique technical challenges, this section focuses on positioning based on wireless local area network (WLAN) radio signals as an inexpensive solution for indoor environments.

2.3.1 IEEE 802.11

What is commonly known as IEEE 802.11 actually refers to the family of standards that includes the original IEEE 802.11 itself, 802.11a, 802.11b, 802.11g and 802.11n. Other common names by which the IEEE standard is known include Wi-Fi and the more generic wireless local area network (WLAN). IEEE 802.11 has become the dominant wireless computer networking standard worked at 2.4GHz with a typical gross bit rate of 11,54,108 Mbps and a range of 50-100m.

Using an existing WLAN infrastructure for indoor location can be accomplished by adding a location server. The basic components of an infrastructure-based location system are shown in Fig.16. The mobile device measures the RSS of signals from the access points (APs) and transmits them to a location server which calculates the location.

There are several approaches for location estimation. The simpler method which is to provide an approximate guess on AP that receives the strongest signal. The mobile node is assumed to be in the vicinity of that particular AP. This method has poor resolution and poor accuracy. The more complex method is to use a radio map. The radio map technique typically utilizes empirical measurements obtained via a site survey, often called the offline phase. Given the RSS measurements, various algorithms have been used to do the match such as *k*-nearest neighbor (*k*-NN), statistical method like the hidden Markov model (HMM). While some systems based on WLAN using RSS requires to receive signals at least three APs and use TDOA algorithm to determine the location.

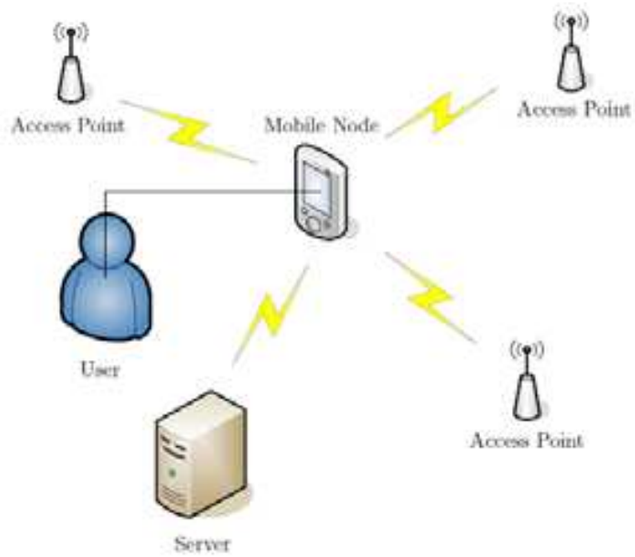

Fig. 16. Typical architecture of WLAN location system

3. Advanced signal processing techniques for wireless positioning

Although many positioning devices and services are currently available, some important problems still remain unsolved. This chapter gives some new ideas, results and advanced signal processing techniques to improve the performance of positioning.

3.1 Computational algorithms of TDOA equations

When TDOA measurements are employed, a set of nonlinear hyperbolic equations has been set up, the next step is to solve these equations and derive the location estimate. Usually, these equations can be solved after being linearized. These algorithms can be grouped into two types: non-iterative methods and iterative methods.

3.1.1 Non-iterative methods

A variety of non-iterative methods for position estimation have been investigated. The most common ones are direct method (DM), least-square (LS) method, Chan method.
When the TDOA is measured, a set of equations can be described as follows.

$$R_{i,1} = c(t_i - t_1) = c\Delta\tau_i = R_i - R_1$$

Where $R_{i,1}$ is the value of range difference from MT to the *i*th RP and the first RP.

Define

$$R_i = \sqrt{(X_i - x)^2 + (Y_i - y)^2}\ , \quad i = 1, \cdots N \tag{8}$$

(X_i, Y_i) is the RP coordinate, (x, y) is the MT location, R_i is the distance between the RP and MT, N is the number of BS, c is the light speed, $\Delta\tau_i$ is the TDOA between the service RP and the *i*th RP_i .
Squaring both sides of (8)

$$R_i^{\,2} = (X_i - x)^2 + (Y_i - y)^2\ , \quad i = 1, \cdots N \tag{9}$$

Substracting (9) for *i*=2,…*N* by (8) for *i*=1

$$X_{i,1}x + Y_{i,1}y = d_{i,1}, i = 2, ...N \tag{10}$$

Where $X_{i,1} = X_i - X_1; Y_{i,1} = Y_i - Y_1$ and $d_{i,1} = ((X_i^2 + Y_i^2) - (X_1^2 + Y_1^2) + R_1^2 - R_i^2)/2$

3.1.1.1 Direct method

It assumes that three RPs are used. The solution to (10) gives:

$$\hat{x} = \frac{Y_{2,1}d_{3,1} - Y_{3,1}d_{2,1}}{X_{3,1}Y_{2,1} - X_{2,1}Y_{3,1}}; \hat{y} = \frac{X_{3,1}d_{2,1} - X_{2,1}d_{3,1}}{X_{3,1}Y_{2,1} - X_{2,1}Y_{3,1}} \tag{11}$$

The solution shows that there are two possible locations. Using a priori information, one of the value is chosen and is used to find out the coordinates.

3.1.1.2 Least square methods

Reordering (10) the terms gives a proper system of linear equations in the form $A\theta = B$, where

$$A = \begin{pmatrix} X_{21} & Y_{21} \\ X_{31} & Y_{31} \end{pmatrix}; \theta = \begin{bmatrix} x \\ y \end{bmatrix}; B = \begin{bmatrix} d_{2,1} \\ d_{3,1} \end{bmatrix}$$

The system is solved using a standard least-square approach:

$$\hat{\theta} = (A^T A)^{-1} A^T B . \tag{12}$$

3.1.1.3 Chan's method

Chan's method (Chan, 1994) is capable of achieving optimum performance. If we take the case of three RPs, the solution of (10) is given by the following relation:

$$\begin{bmatrix} x \\ y \end{bmatrix} = -\begin{pmatrix} X_{21} & Y_{21} \\ X_{31} & Y_{31} \end{pmatrix}^{-1} \left\{ \begin{bmatrix} d_{21} \\ d_{31} \end{bmatrix} \times R_1 + 0.5 \times \begin{bmatrix} d_{21}^2 - K_2 + K_1 \\ d_{31}^2 - K_3 + K_1 \end{bmatrix} \right\} \tag{13}$$

Where

$K_i = X_i^2 + Y_i^2, i = 1,2,3$

3.1.2 Iterative method

Taylor series expansion method is an iterative method which starts with an initial guess which is in the condition of close to the true solution to avoid local minima and improves the estimate at each step by determining the local linear least-squares.

Eq. (10) can be rewritten as a function

$$f_i(x,y) = \sqrt{(x - X_{i+1})^2 + (y - Y_{i+1})^2} - \sqrt{(x - X_1)^2 + (y - Y_1)^2} \qquad i = 1, \cdots N\text{-}1 \tag{14}$$

Let $\hat{t}_i$ be the corresponding time of arrival at BS_i. Then,

$$f_i(x,y) = \hat{d}_{i+1,1} + \varepsilon_{i+1,1} \qquad i = 1, \cdots N\text{-}1 \tag{15}$$

Where

$$\hat{d}_{i+1,1} = c(\hat{t}_{i+1} - \hat{t}_1) \tag{16}$$

$\varepsilon_{i,1}$ is the corresponding range differences estimation error with covariance R.

If (x_0, y_0) is the initial guess of the MS coordinates, then

$$x = x_0 + \delta_x, \quad y = y_0 + \delta_y \tag{17}$$

Expanding Eq. (15) in Taylor series and retaining the first two terms produce

$$f_{i,0} + a_{i,1}\delta_x + a_{i,2}\delta_y \approx \hat{d}_{i+1,1} + \varepsilon_{i+1,1} \qquad i = 1, \cdots N - 1 \tag{18}$$

Where

$$
\begin{aligned}
f_{i,0} &= f_i(x_0, y_0) \\
a_{i,1} &= \left.\frac{\partial f_i}{\partial x}\right|_{x_0, y_0} = \frac{X_1 - x_0}{\hat{d}_1} - \frac{X_{i+1} - x_0}{\hat{d}_{i+1}} \\
\hat{d}_i &= \sqrt{(x_0 - X_i)^2 + (y_0 - Y_i)^2} \\
a_{i,2} &= \left.\frac{\partial f_i}{\partial y}\right|_{x_0, y_0} = \frac{Y_1 - y_0}{\hat{d}_1} - \frac{Y_{i+1} - y_0}{\hat{d}_{i+1}}
\end{aligned}
\tag{19}
$$

Eq. (18) can be rewritten as

$$
\mathrm{A}\delta = \mathrm{D} + \mathrm{e} \tag{20}
$$

Where

$$
\mathrm{A} = \begin{bmatrix} a_{1,1} & a_{1,2} \\ a_{2,1} & a_{2,2} \\ \vdots & \vdots \\ a_{N-1,1} & a_{N-1,2} \end{bmatrix}, \quad \delta = \begin{bmatrix} \delta_x \\ \delta_y \end{bmatrix}
$$

$$
\mathrm{D} = \begin{bmatrix} \hat{d}_{2,1} - f_{1,0} \\ \hat{d}_{3,1} - f_{2,0} \\ \vdots \\ \hat{d}_{N,1} - f_{N-1,0} \end{bmatrix}, \quad \mathrm{e} = \begin{bmatrix} \varepsilon_{2,1} \\ \varepsilon_{3,1} \\ \vdots \\ \varepsilon_{N,1} \end{bmatrix}
$$

The weighted least square estimator for (20) produces

$$
\delta = \left[\mathrm{A}^{\mathrm{T}}\mathrm{R}^{-1}\mathrm{A}\right]^{-1}\mathrm{A}^{\mathrm{T}}\mathrm{R}^{-1}\mathrm{D} \tag{21}
$$

R is the covariance matrix of the estimated TDOAs.

Taylor series method starts with an initial guess (x_0, y_0), in the next iteration, (x_0, y_0) are set to $(x_0 + \delta_x, y_0 + \delta_y)$ respectively. The whole process is repeated until (δ_x, δ_y) are sufficiently small. The Taylor series method can provide accurate results, however the convergence of the iterative process depends on the initial value selection. The recursive computation is intensive since least square computation is required in each iteration.

3.1.3 Steepest decent method

From the above analysis, the convergence of Taylor series expansion method and the convergence speed directly depends on the choice of the MT initial coordinates. This iterative method must start with an initial guess which is in the condition of close to the true solution to avoid local minima. Selection of such a starting point is not simple in practice.

To solve this problem, steepest decent method with the properties of fast convergence at the initial iteration and small computation complexity is applied at the first several iterations to

get a corrected MT coordinates which are satisfied to Taylor series expansion method. The algorithm is described as follows.
Eq. (18) can be rewritten as

$$\varphi_i(x,y) = f_i(x,y) - \hat{d}_{i+1,1} + \varepsilon_{i+1,1} \qquad i = 1,\cdots N\text{-}1 \tag{19}$$

Construct a set of module functions from Eq. (18)

$$\Phi(x,y) = \sum_{i=1}^{N-1} \left[\varphi_i(x,y)\right]^2 \tag{20}$$

The solution to Eq. (18) is translated to compute the point of minimum Φ. In geometry, $\Phi(x,y)$ is a three-dimension curve, the minimum point equals to the tangent point between $\Phi(x,y)$ and xOy. In the region D of $\Phi(x,y)$, any point is passed through by an equal high line. If starting with an initial guess (x_0,y_0) in the region D, declining $\Phi(x,y)$ in the direction of steepest descent until $\Phi(x,y)$ declines to minimum, and then we can get the solution.
Usually, the normal direction of an equal high line is the direction of the gradient vector of $\Phi(x,y)$ which is denoted by

$$G = \left(\frac{\partial \Phi}{\partial x}, \frac{\partial \Phi}{\partial y}\right)^{\mathrm{T}} \tag{21}$$

The opposite direction to the gradient vector is the steepest descent direction.
Given (x_0,y_0) is an approximate solution, compute the gradient vector at this point

$$G_0 = (g_{10}, g_{20})^{\mathrm{T}}$$

Where

$$\begin{cases} g_{10} = \left.\dfrac{\partial \Phi}{\partial x}\right|_{(x_0,y_0)} = 2\left[\sum\limits_{i=1}^{N-1} \left(\dfrac{\partial \varphi_i}{\partial x}\right)\varphi_i\right]_{(x_0,y_0)} \\ g_{20} = \left.\dfrac{\partial \Phi}{\partial y}\right|_{(x_0,y_0)} = 2\left[\sum\limits_{i=1}^{N-1} \dfrac{\partial \varphi_i}{\partial y}\right]\varphi_i]_{(x_0,y_0)} \end{cases} \tag{22}$$

Then, start from (x_0,y_0), cross an appropriate step-size in the direction of $-G_0$, λ is the step-size parameter, get a new point (x_1,y_1)

$$\begin{cases} x_1 = x_0 - \lambda g_{10} \\ y_1 = y_0 - \lambda g_{20} \end{cases} \tag{23}$$

Choose an appropriate λ in order to let (x_1,y_1) be the relative minimum in $-G_0$,

$$\Phi(x_1,y_1) \approx \min\{\Phi(x_0 - \lambda g_{10}, y_0 - \lambda g_{20})\}$$

In order to fix on another approximation close to (x_0, y_0), expand $\varphi_i(x_0 - \lambda g_{10}, y_0 - \lambda g_{20})$ at (x_0, y_0), omit λ^2 high order terms, get the approximation of Φ

$$\Phi(x_0 - \lambda g_{10}, y_0 - \lambda g_{20}) = \sum_{i=1}^{N-1} [\varphi_i(x_0 - \lambda g_{10}, y_0 - \lambda g_{20})]^2$$

$$\approx \{ \sum_{i=1}^{N-1} (\varphi_i)^2 - 2\lambda [\sum_{i=1}^{N-1} \varphi_i (g_{10} \frac{\partial \varphi_i}{\partial x} + g_{20} \frac{\partial \varphi_i}{\partial y})] + \lambda^2 [\sum_{i=1}^{N-1} (g_{10} \frac{\partial \varphi_i}{\partial x} + g_{20} \frac{\partial \varphi_i}{\partial y})^2] \}_{(x_0, y_0)}$$

Let $\partial\Phi / \partial\lambda = 0$,

$$\lambda = \left[\frac{\sum_{i=1}^{N-1} \varphi_i (g_{10} \frac{\partial \varphi_i}{\partial x} + g_{20} \frac{\partial \varphi_i}{\partial y})}{\sum_{i=1}^{N-1} (g_{10} \frac{\partial \varphi_i}{\partial x} + g_{20} \frac{\partial \varphi_i}{\partial y})^2} \right]_{(x_0 \cdot y_0)} \tag{24}$$

Subtract Eq. (24) from Eq. (23), we obtain a new (x_1, y_1), and regard this as a relative minimum point of Φ in the direction of $-G_0$, then start at this new point (x_1, y_1), update the position estimate according to the above steps until Φ is sufficiently small.

In general, the convergence of steepest descent method is fast when the initial guess is far from the true solution, vice versa. Taylor series expansion method has been widely used in solving nonlinear equations for its high accuracy and good robustness. However, this method performs well under the condition of close to the true solution, vice versa. Therefore, hybrid optimizing algorithm (HOA) is proposed combining both Taylor series expansion method and steepest descent method, taking great advantages of both methods, optimizing the whole iterative process, improving positioning accuracy and efficiency.

In HOA, at the beginning of iteration, steepest descent method is applied to let the rough initial guess close to the true solution. Then, a further precise adjustment is implemented by Taylor series expansion method to make sure that the final estimator is close enough to the true solution. HOA has the properties of good convergence and improved efficiency. The specific flow is

1. Give a free initial guess (x_0, y_0), compute $i = 1 \cdots N-1$, $\frac{\partial \varphi_i}{\partial x}, \frac{\partial \varphi_i}{\partial y}$
2. Compute the gradient vector g_{10}, g_{20} at the point (x_0, y_0) from Eq. (22)
3. Compute λ from Eq. (24)
4. Compute (x_1, y_1) from Eq. (23)
5. If $\Phi \approx 0$, stop; otherwise, substitute (x_1, y_1) for (x_0, y_0), iterate (2)(3)(4)(5)
6. Compute $\hat{d}_{i+1,1}$ when $i = 1 \cdots N-1$ from Eq. (16)
7. Compute $\hat{d}_1, \hat{d}_{i+1}, f_{i,0}, a_{i,1}, a_{i,2}$ when $i = 1 \cdots N-1$ from Eq. (19)
8. Compute δ from Eq. (21)
9. Continually refine the position estimate from (7)(8)(9) until δ satisfies the accuracy

According to the above flow, the performance of the proposed HOA is evaluated via Matlab simulation software. In the simulation, we model a cellular system with one central BS and

two other adjacent BS. More assistant BS can be utilized for more accuracy, however, in cellular communication systems, one of the Main design philosophies is to make the link loss between the target mobile and the home BS as small as possible, while the other link loss as large as possible to reduce the interference and to increase signal-to-interference ratio for the desired communication link. This design philosophy is not favorable to position location (PL), and leads to the main problems in the current PL technologies, i.e. hearability and accuracy. Considering the balance between communication link and position accuracy, two assistant BS is chose. We assume that the coordinates of central BS is (x1=0m ; y1=0m), the two assistant BS coordinates is (x2=2500m ; y2=0m); (x3=0m ; y3=2500m) respectively, MS coordinates is (x=300;y=400). A comparison of HOA and Taylor series expansion method is presented.

A lot of simulation computation demonstrates: there are 3 situations. The first one is that HOA is more accuracy and efficiency under the precondition of the same initial guess and the same measured time. In the second situation, HOA is more convergence to any initial guess than Taylor series expansion method under the precondition of the same initial guess and the same measured time. In the third situation, at the prediction of inaccurate measurements, the same initial guess, HOA is proved to be more accuracy and efficiency. The simulation results are given in Tables 3,4,5 respectively.

As shown in Table 3, the steepest decent method performs much better at the convergence speed. Indeed, the location error is smaller than Taylor series expansion method for 10^3. Meanwhile, the computation efficiency is improved by 23.35%. The result is that HOA is more accuracy and efficiency.

As shown in Table 4, when the initial guess is far from the true location, Taylor series expansion method is not convergent while HOA is still convergent which declines the constraints of the initial guess.

As shown in Table 5, when the measurements are inaccurate, the HOA location error is smaller than Taylor series expansion method for 10 times. Meanwhile, the computation efficiency is improved by 23.14%.

algorithms	Iterative results(m)	errors(m)	time(ms)
HOA	x =299.9985 y =400.0006	xx =-0.0015 yy =0.0006	0.374530
Taylor	x=301.1 y=400.4482	xx=1.1000 yy=0.4482	0.488590

Table 3. Comparison of HOA and Taylor series expansion method when the initial guess is close to the true solution and the measured time is accurate

algorithms	Iterative results(m)	errors(m)	time(ms)
HOA	x =299.9985 y =400.0006	xx =-0.0015 yy =0.0006	1.025930
Taylor	x =+∞ y =+∞	Not convergent	

Table 4. Comparison of HOA and Taylor series expansion method when the initial guess is far from the true solution and the measured time is accurate

algorithms	Iterative results(m)	errors(m)	time(ms)
HOA	x= 301.1297 y= 400.4492	xx=1.1297 yy=0.4492	0.376400
Taylor	x =317.8 y =396.0549	xx=17.8000 yy=-3.9451	0.489680

Table 5. Comparison of HOA and Taylor series expansion method when the initial guess is the same and the measured time is inaccurate

3.2 Data fusion techniques

Date fusion techniques include system fusion and measurement data fusion (Sayed, 2005). For example, a combination of GPS and cellular networks can provide greater location accuracy, and that is one kind of system fusion. Measurement data fusion combines different signal measurements to improve accuracy and coverage. This section mainly concerns how to use measurement data fusion techniques to solve problems in cellular-based positioning system.

3.2.1 Technical challenges in cellular-based positioning

The most popular cellular-based positioning method is multi-lateral localization. In such positioning system, there are two major challenges, non-line-of-sight (NLOS) propagation problem and hearability.

A. Hearability problem

In cellular communication systems, one of the main design philosophies is to make the link loss between the target mobile and the home BS as small as possible, while the other link loss as large as possible to reduce the interference and to increase signal to noise ratio for the desired communication link. In multi-lateral localization, the ability of multiple base stations to hear the target mobile is required to design the localization system, which deviates from the design of wireless communication system , and this phenomenon is referred as hearability (Prretta, 2004).

B. The non-line-of-sight propagation problem

Most location systems require line-of-sight radio links. However, such direct links do not always exist in reality because the link is always attenuated or blocked by obstacles. This phenomenon, which refers as the NOLS error, ultimately translates into a biased estimate of the mobile's location (Cong, 2001).

As illustrated by the signal transmission between BS7 and MS in Fig.17. A NLOS error results from the block of direct signal and the reflection of multipath signals. It is the extra distance that a signal travels from transmitter to receiver and as such always has a nonnegative value. Normally, NLOS error can be described as a deterministic error, a Gaussian error, or an exponentially distributed error.

In order to demonstrate the performance degradation of a time-based positioning algorithm due to NLOS errors, taking the TOA method as an example. The least square estimator used for MS location is of the following form

$$\hat{\mathbf{x}} = \arg\min \sum_{i \in S} (r_i - \|\mathbf{x} - \mathbf{X}_i\|)^2 \tag{25}$$

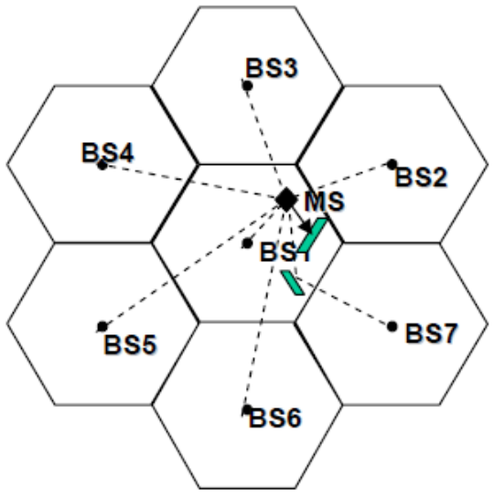

Fig. 17. NLOS error

$$r_i = L_i + n_i + e_i, \quad i = 1,2,...N \tag{26}$$

Where r is the range observation, L is LOS range, n is receiver noise, e is NLOS error.

$$\mathbf{r = L + n + e} \tag{27}$$

If the true MS location is used as the initial point in the least square solution, the range measurements can be expressed via a Taylor series expansion as

$$\mathbf{r} \approx \mathbf{L} + \mathbf{G}\begin{bmatrix} \Delta x \\ \Delta y \end{bmatrix} \tag{28}$$

$$\begin{bmatrix} \Delta x \\ \Delta y \end{bmatrix} = (\mathbf{G}^{\mathbf{T}}\mathbf{G})^{-1}\mathbf{G.n} + (\mathbf{G}^{\mathbf{T}}\mathbf{G})^{-1}\mathbf{G.e} \tag{29}$$

Where G is the design matrix, and $[\Delta x, \Delta y]$ is the MS location error. Because NLOS errors are much larger than the measurement noise, the positioning errors result mainly from NLOS errors if NLOS errors exist.

3.2.2 Data fusion architecture

The underlying idea of data fusion is the combination of disparate data in order to obtain a new estimate that is more accurate than any of the individual estimates. This fusion can be accomplished either with raw data or with processed estimates. One promising approach to the general data fusion problem is represented by an architecture that was developed in 1992 by the data fusion working group of the joint directors of laboratories (JDL) (Kleine-Ostmann, 2001). This architecture is comprised of a preprocessing stage, four levels of fusion and data management functions. As a refinement of this architecture, Hall proposed a hybrid approach to data fusion of location information based on the combination of level one and level two fusion (Kleine-Ostmann, 2001).

Based on the JDL model and its specialization to first and second level hybrid data fusion, an architecture for the position estimation problem in cellular networks is constructed. Fig. 18. shows the data fusion model that uses four level data fusion.

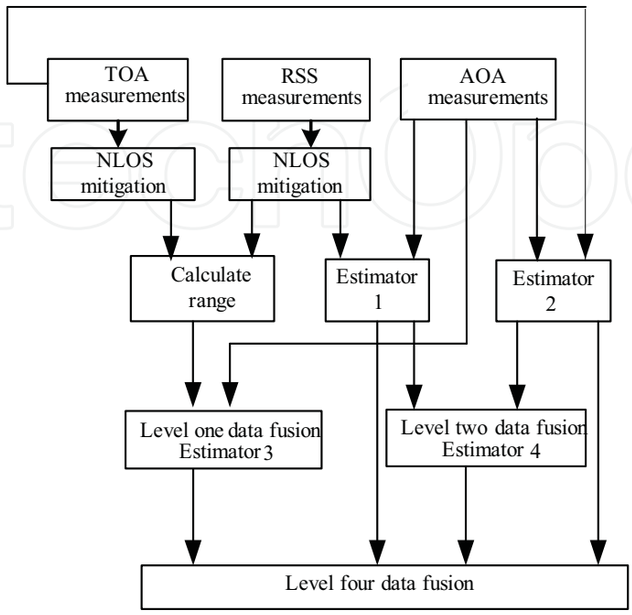

Fig. 18. Data fusion model

Position estimates are obtained by four different approaches in this model. The first approach uses TOA/AOA hybrid method. The second position estimate is based on RSS /AOA hybrid method. The other two estimates are obtained by level one and level 2 data fusion methods.

A. Level one fusion

Firstly, we use the method shown in (Wylie, 1996) to mitigate TOA NLOS error and calculate the LOS distance d_{TOA}. As the same way, we mitigate RSS NLOS error and calculate the LOS distance d_{RSS}. Then, the independent d_{TOA} and d_{RSS} are fused into d. The derivation of d is below.

Let

$$\begin{cases} \mathrm{Var}(d_{\mathrm{TOA}}) = \sigma_{\mathrm{TOA}}^2 \\ \mathrm{Var}(d_{\mathrm{RSS}}) = \sigma_{\mathrm{RSS}}^2 \end{cases}$$

Define,

$$d = f(d_{\mathrm{TOA}}, d_{\mathrm{RSS}}) = ad_{\mathrm{TOA}} + bd_{\mathrm{RSS}} \tag{30}$$

The constrained minimization problem is described as (31)

$$\begin{aligned} &\arg_{\min}[\mathrm{Var}(d)] = \arg_{\min}[\mathrm{E}(d - \bar{d})^2] \\ &a + b = 1 \end{aligned} \tag{31}$$

By using Lagrange Multipliers, the solution of (31) is obtained as (32)

$$a = \frac{\sigma_{\mathrm{RSS}}^2}{\sigma_{\mathrm{RSS}}^2 + \sigma_{\mathrm{TOA}}^2},\ b = \frac{\sigma_{\mathrm{TOA}}^2}{\sigma_{\mathrm{TOA}}^2 + \sigma_{\mathrm{RSS}}^2} \tag{32}$$

The data fusion result is given by (33)

$$d = \frac{\sigma_{\mathrm{RSS}}^2 d_{\mathrm{TOA}} + \sigma_{\mathrm{TOA}}^2 d_{\mathrm{RSS}}}{\sigma_{\mathrm{TOA}}^2 + \sigma_{\mathrm{RSS}}^2} \tag{33}$$

Using (32)(33), the variance of d is

$$\mathrm{Var}(d) = (\frac{1}{\sigma_{\mathrm{TOA}}^2} + \frac{1}{\sigma_{\mathrm{RSS}}^2})^{-1} \tag{34}$$

Therefore,

$$\begin{aligned} \mathrm{Var}(d) &\le (\frac{1}{\sigma_{\mathrm{TOA}}^2})^{-1} = \mathrm{Var}(d_{\mathrm{TOA}}) \\ \mathrm{Var}(d) &\le (\frac{1}{\sigma_{\mathrm{RSS}}^2})^{-1} = \mathrm{Var}(d_{\mathrm{RSS}}) \end{aligned} \tag{35}$$

So, the data fusion estimator is more accurate than estimator 1 or 2.

B. Level two fusion

By utilizing the result proved in (32)(33)(34), the estimator 4 fused solution and its variance are of the following equations.

$$x_{\mathrm{C}} = \frac{\sigma_{\mathrm{TOA/AOA}}^2 x_{\mathrm{RSS/AOA}} + \sigma_{\mathrm{RSS/AOA}}^2 x_{\mathrm{TOA/AOA}}}{\sigma_{\mathrm{TOA/AOA}}^2 + \sigma_{\mathrm{RSS/AOA}}^2} \tag{36}$$

$$\sigma_{\mathrm{C}}^2 = (\frac{1}{\sigma_{\mathrm{TOA/AOA}}^2} + \frac{1}{\sigma_{\mathrm{RSS/AOA}}^2})^{-1} \tag{37}$$

Where $x_{\mathrm{RSS/AOA}}$ and variance $\sigma_{\mathrm{RSS/AOA}}^2$ are the mean and variance of estimator 1, $x_{\mathrm{TOA/AOA}}$ and $\sigma_{\mathrm{TOA/AOA}}^2$ are the mean and variance of estimator 2, x_{C} and σ_{C}^2 are the mean and variance of estimator 4.

C. Level three fusion

In general, the estimate that exhibits the smallest variance is considered to be the most reliable estimate. However, the choice cannot be based solely on variance. In a poor signal propagation situation when the MS is far from BSs, the RSS estimate becomes mistrust.

3.2.3 Single base station positioning algorithm based on data fusion model

To solve the problem, a single home BS localization method is proposed in this paper. In (Wylie, 1996), a time-history-based method is proposed to mitigate NLOS error. Based on

this method, a novel single base station positioning algorithm based on data fusion model is established to improve the accuracy and stability of localization.
Fig.19. illustrates the geometry fundamental of this method. The MT coordinates (x, y) is simply calculated by (38)

$$\begin{aligned} x &= d\cos\alpha \\ y &= d\sin\alpha \end{aligned} \tag{38}$$

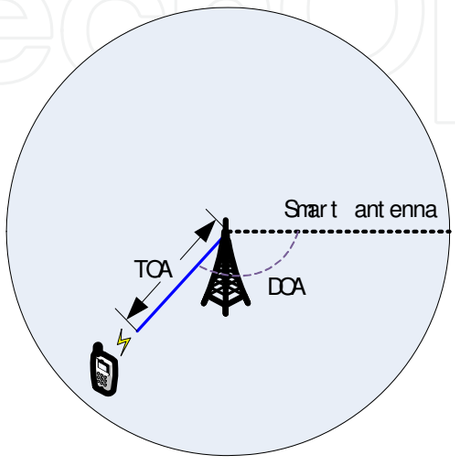

Fig. 19. Geometry of target coordinates (x, y)

The MT localization is determined by d and α where d denotes the line-of-sight (LOS) distance between the MT and the home BS, α denotes the signal direction from the home BS to the TM. The above two parameters are important for localization accuracy. Data fusion model discussed above can be utilized to get a more accurate localization.
In this section, we present some examples to demonstrate the performance of the proposed method. We suppose the MT's trajectory is x=126.9+9.7t , y=286.6+16.8t, sampling period is 0.05s, 200 samples are taken, 50 random tests are taken in one sample. The velocity is constant at $v_x = 9.7\text{m/s}$, $v_y = 16.8\text{m/s}$. The TOA measurements error is Gaussian random variable with zero mean and standard variance 20, NLOS error is exponential distribution with mean 100. RSS medium-scale path loss is a zero mean Gaussian distribution with standard deviation 20 and small-scale path loss is a Rayleigh distribution with $\sigma_{ss}^2 = 79.7885$. The home BS is located at (0,0).
Simulation 1, when the NLOS and measurements error are added to the TOA, we utilize (Wylie, 1996) to reconstruct LOS. Fig.20. shows the results. From the results, we can see that NLOS error is the major effect to bias the true range up to 900m. Due to NLOS, at most of the time, the measurements are much larger than the true range. After the reconstruction, the corrected range is near the true range and float around the true range.
Simulation 2, when the medium-scale path loss and small-scale path loss are added to the RSS, we utilize (Wylie, 1996) to reconstruct LOS. Fig.21. shows the results. From the results, we can see that the small-scale error (NLOS error) is the major effect to bias the true range up to 700m. Due to the NLOS, at most of the time, the measurements are much larger than the true range. After the reconstruction, the corrected range is near the true range and float around the true range.

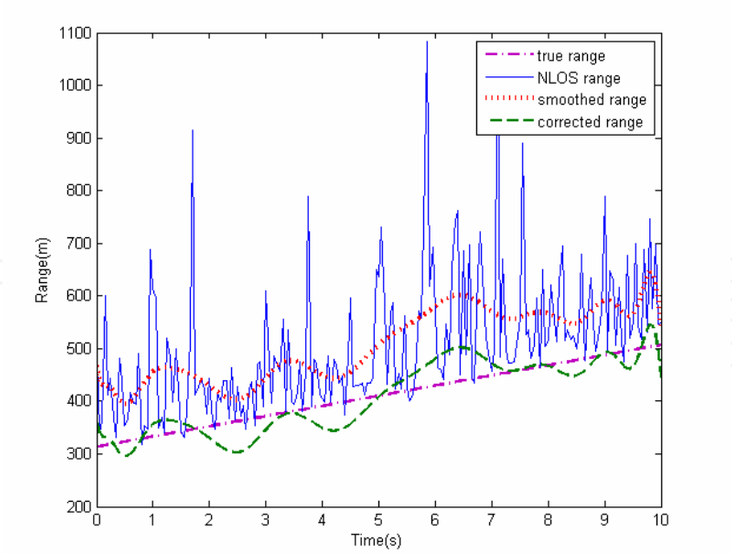

Fig. 20. TOA LOS reconstruction from NLOS measurements

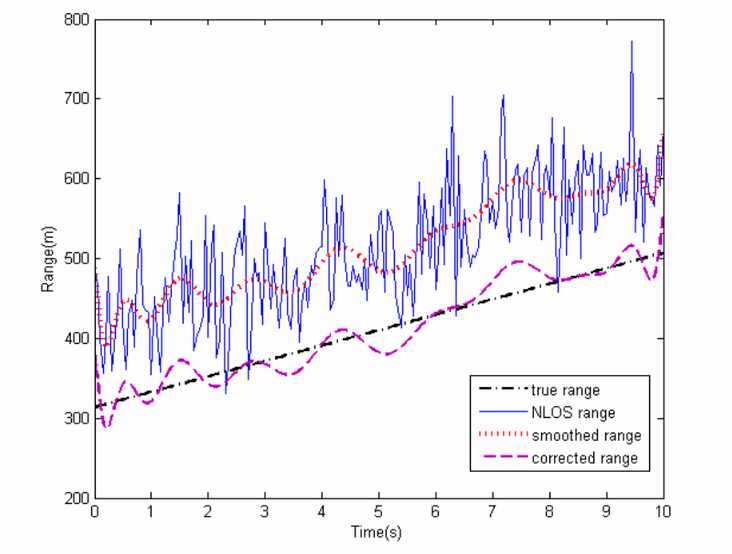

Fig. 21. RSS LOS reconstruction from NLOS measurements

Simulation 3 is about the localization improvement. The results are shown in Fig.22. It indicates that the standard variance of the proposed method is smaller than any of TOA or RSS. HLMR technique is able to significantly reduce the estimation bias when compared to the classic NLOS mitigation method shown by (Wylie, 1996). By statistical calculation, the mean of TOA standard variance by (Wylie, 1996) is 37.382m, while the data fusion aided method is 17.695m. The stability is more than one time higher. Fig.23. demonstrates the Euclidean distance between the true range and estimation range by data fusion based method, TOA and AOA. The mathematical expressions are given in (39)(40)(41). By statistical calculation, the Euclidean distance of TOA is 37.44, the proposed method is 3.1318 which is ten times more accurate.

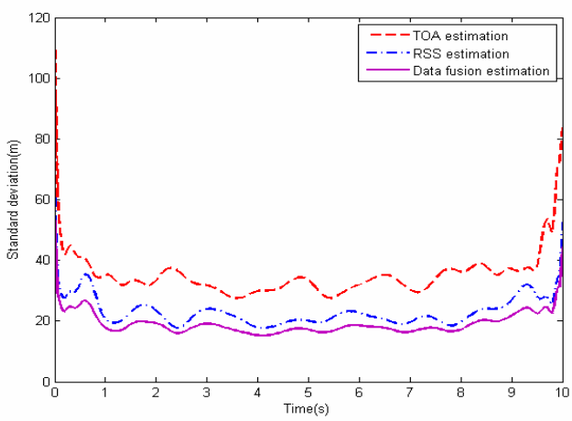

Fig. 22. Standard variance of estimation range

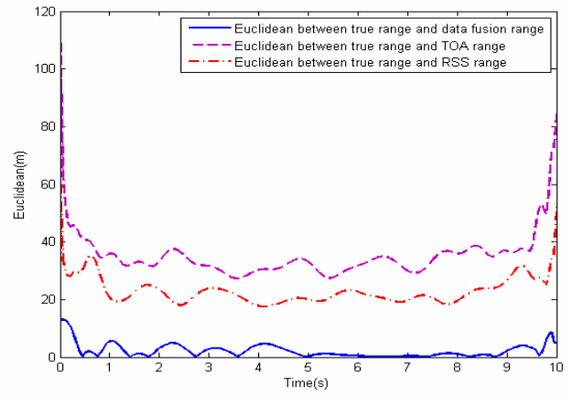

Fig. 23. Euclidean distance between true range and estimation range

$$\|\mathbf{r}-\mathbf{d}\| = \sqrt{\sum_{i=1}^{N}(r_i - d_i)^2} \tag{39}$$

$$\|\mathbf{r}-\mathbf{d}_{\mathbf{TOA}}\| = \sqrt{\sum_{i=1}^{N}(r_i - d_{\mathrm{TOA}_i})^2} \tag{40}$$

$$\|\mathbf{r}-\mathbf{d}_{\mathbf{RSS}}\| = \sqrt{\sum_{i=1}^{N}(r_i - d_{\mathrm{RSS}_i})^2} \tag{41}$$

3.3 UWB precise real time location system

Reliable and accurate indoor positioning for moving users requires a local replacement for satellite navigation. Ultra WideBand (UWB) technology is particularly suitable for such local systems, for its good radio penetration through structures, the rapid set-up of a stand-alone system, tolerance of high levels of reflection, and high accuracy even in the presence of severe multipath (Porcino, 2003).

3.3.1 UWB localization challenges

UWB technology is defined by the Federal Communications Commission (FCC) as any wireless transmission scheme that occupies a fractional bandwidth $W / f_c \geq 20\%$ where W is the transmission bandwidth and fc is the band center frequency, or more than 500 MHz of absolute bandwidth. FCC approved the deployment of UWB on an unlicensed basis in the 3.1-10.6GHz band with limited power spectral density as shown in Fig.24.

UWB signal is a kind of signals which occupies several GHz of bandwidth by modulating an impulse-like waveform. A typical baseband UWB signal is Gaussian monocycle obtained by differentiation of the standard Gaussian waveform (Roy, 2004). A second derivative of Gaussian pulse is given by

$$p(t) = A[1 - 4\pi(\frac{t}{T_d})^2]e^{-2\pi(\frac{t}{T_d})^2} \tag{42}$$

Where the amplitude A can be used to normalize the pulse energy. Fig.25 shows the time domain waveform of (42). From Fig.25, we see that the duty cycle (the pulse duration divided by the pulse period) is really small. In other aspect of view, UWB signal is sparse in time domain. The Fourier transform (Fig.26) is occupied from near dc up to the system bandwidth $B_S \approx 1/T_d$.

A. CRLB for time delay estimation

The CRLB defines the best estimation performance, defined as the minimum achievable error variance, which can be achieved by using an ideal unbiased estimator. It is a valuable tool in evaluating the potential of UWB signals for TOA estimation. In this section, we will derive the expression of the CRLB of TOA estimation for UWB signals.

Consider the signal in (42) is sampled with a sampling period T_s. The sequence of the samples is written as

$$r_n = s_n(\tau) + w_n \tag{43}$$

The joint probability of r_n conditioned to the knowledge of delay τ :

$$p(r_n|\tau) = (2\pi\sigma^2)^{-\frac{N}{2}} \exp(-\frac{1}{2\sigma^2}\sum_{n=1}^{N}(r_n - s_n(\tau)^2)) \tag{44}$$

Where N is the number of samples, σ^2 is the variance of r_n.

In order to get the continuous probability of (44)

$$\begin{aligned} p(r|\tau) &= \lim_{N\to+\infty} p(r_n|\tau) \\ &= (2\pi\sigma^2)^{-\frac{N}{2}} \exp(-\frac{1}{2\sigma^2}\int_0^T (r(t) - s(t;\tau))^2 dt) \end{aligned} \tag{45}$$

The log-likelihood function of (45)

$$\ln p = \ln(2\pi\sigma^2)^{-\frac{N}{2}} - \frac{1}{2\sigma^2}\int_0^T (r(t) - s(t;\tau))^2 dt \tag{46}$$

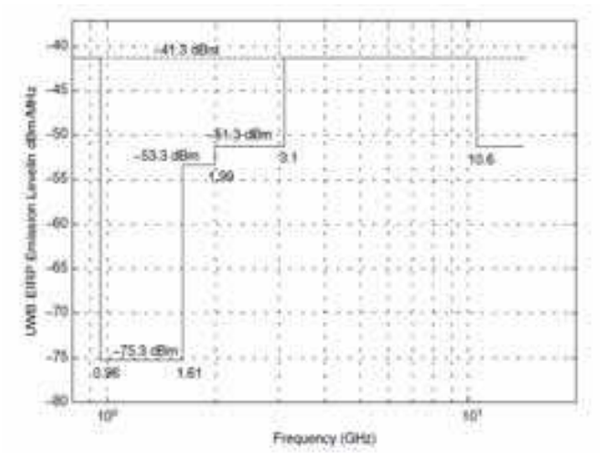

Fig. 24. UWB spectral mask

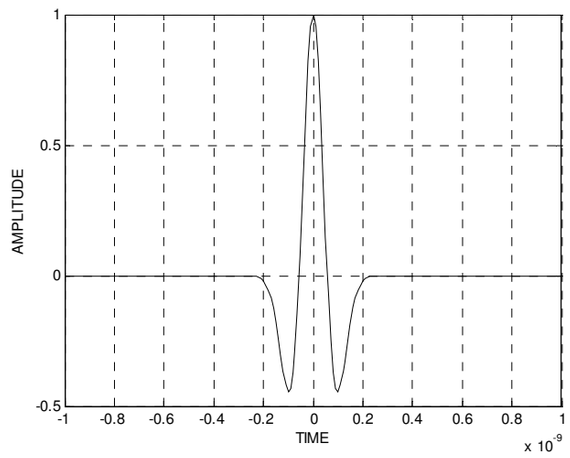

Fig. 25. UWB signal in time domain

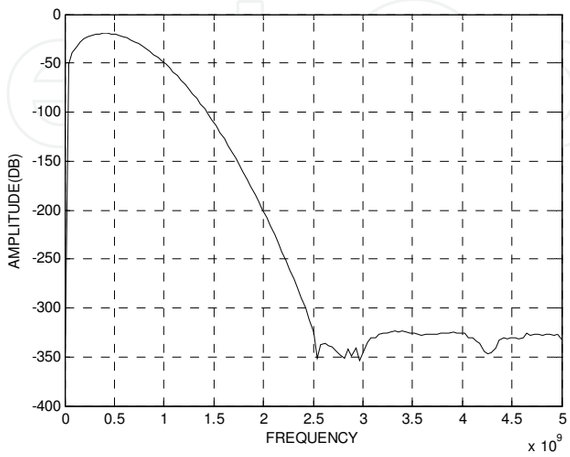

Fig. 26. UWB signal in frequency domain

The second differentiation of (46) is

$$\frac{\partial^2 \ln p}{\partial^2 \tau} = \frac{1}{\sigma^2}(\int_0^T s''(t;\tau)(r(t) - s(t;\tau))dt + \int_0^T -(s'(t;\tau))^2 dt) \tag{47}$$

The average value of (47)

$$E(\frac{\partial^2 \ln p}{\partial^2 \tau}) = -\frac{1}{\sigma^2}\int_0^T (s'(t;\tau))^2 dt$$

The minimal achievable variance for any unbias estimation (CRLB) is thus:

$$\begin{aligned} \sigma_t^2 &= -\frac{1}{E(\frac{\partial^2 \ln p}{\partial^2 \tau})} = \frac{\sigma^2}{\int_0^T (s'(t;\tau))^2 dt} \\ &= \frac{\sigma^2}{\int_0^T s^2(t;\tau)dt} \cdot \frac{\int_0^T s^2(t;\tau)dt}{\int_0^T (s'(t;\tau))^2 dt} \\ &= (\frac{E}{N})^{-1}.\beta^2 \end{aligned} \tag{48}$$

Where

$$\begin{aligned} \beta^2 &= \frac{\int_0^T s^2(t;\tau)dt}{\int_0^T (s'(t;\tau))^2 dt} = \frac{\int S^2(f;\tau)df}{\int f^2 S^2(f;\tau)df} \\ &\geq \frac{\int S^2(f;\tau)df}{\int f^2 df . \int S^2(f;\tau)df} = \frac{1}{\int f^2 df} \end{aligned} \tag{49}$$

The equality holds if $f = kS(f;\tau)$, where k is an arbitrary constant. E/N is the signal to noise ratio, and $S(f)$ is the fourier transform of the transmitted signal.
Inequation (49) shows that the accuracy of TOA is inversely proportional to the signal bandwidth. Since UWB signals have very large bandwidth, this property allows extremely accurate TOA estimation. UWB signal is very suitable for TOA estimation. However, there are many challenges in developing such a real time indoor UWB positioning system due to the difficulty of large bandwidth sampling technique and other challenges.

3.3.2 Compressive sensing based UWB sampling method

As discussed above, due to a large bandwidth of a UWB signal, it can't be sampled at receiver directly, how to compress and reconstruct the signal is a problem. To solve this problem, this section gives a new perspective on UWB signal sampling method based on Compressive Sensing (CS) signal processing theory (Candès, 2006; Candès,2008; Richard, 2007).

CS theory indicates that certain digital signals can be recovered from far fewer samples than traditional methods. To make this possible, CS relies on two principles: sparsity and incoherence.

Sparsity expresses the idea that the number of freedom degrees of a discrete time signal may be much smaller than its length. For example, in the equation x=ψα, by K-sparse we mean that only $K \leq N$ of the expansion coefficients α representing x=ψα are nonzero. By compressible we mean that the entries of a, when sorted from largest to smallest, decay rapidly to zero. Such a signal is well approximated using a K-term representation.

Incoherent is talking about the coherence between the measurement matrix ψ and the sensing matrix Φ. The sensing matrix is used to convert the original signal to fewer samples by using the transform y=Φx =ΦΨα as shown in Fig.27. The definition of coherence is $\mu(\Phi,\Psi) = \sqrt{n}.\max_{1\le k,j\le n}\left|\left\langle \phi_k,\varphi_j \right\rangle\right|$. It follows from linear algebra that is $\mu(\Phi,\Psi)\in[1,\sqrt{n}]$. In CS, it concerns about low coherence pairs. The results show that random matrices are largely incoherent with any fixed basis Ψ. Gaussian or ±1 binaries will also exhibit a very low coherence with any fixed representation Ψ.

Since M <N, recovery of the signal x from the measurements y is ill-posed; however the additional assumption of signal sparsity in the basis Ψ makes recovery possible and practical.

The signal can be recovered by solving the following convex program as shown in Fig. 27.

α = arg min $||\alpha||_1$ s.t. y = ΦΨα.

And M should obey $M \geq C.\mu^2(\Phi,\Psi).K.\log N$, where C is a small constant, K is the number of non-zero elements, N is the length of the original signal.

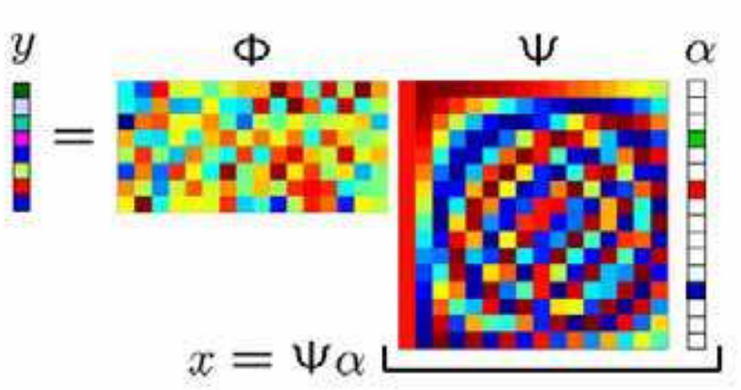

Fig. 27. Compressive sensing transform

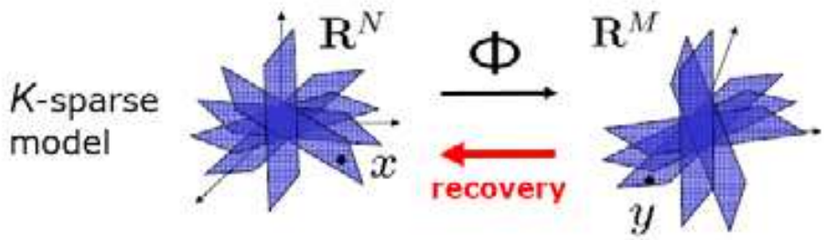

Fig. 28. Signal recovery algorithm

we utilize the temporal sparsity property of UWB signals and CS technique. There are three key elements needed to be addressed in the use of CS theory into UWB signal sampling: 1) How to find a space in which UWB signals have sparse representation 2) How to choose random measurements as samples of sparse signal 3) How to reconstruct the signal.
CS is mainly concerned with low coherent pairs. How to find a good pair of Φ and Ψ in which UWB signals have sparse representation is the problem we need to solve. Since UWB signal is sparse in time domain, we choose Ψ is spike basis $\phi_k(t) = \delta(t-k)$ and Φ is random Gaussian matrix.
The mathematical principle can be formulated as

$$\mathbf{s} = \mathbf{G}.\mathbf{E}.p(t)\big|_{t=kT} + \mathbf{n} \quad k=1\ldots N \tag{50}$$

Where **s** is the sensing vector, **G** is random Gaussian matrix, **E** is spike matrix, $p(t)\big|_{t=kT}$ is the Nyquist samples with sample period T, total samples N. **n** is the additive noise vector with bounded energy $\|\mathbf{n}\|_2 \le \varepsilon$.

The coherence between measurement matrix **E** and sensing matrix **G** is near 1. **G** matrix is largely incoherent with **E**. Therefore, in our method, the precondition of sparsity and incoherent are satisfied.

$$u(\mathbf{G},\mathbf{E}) = \sqrt{n}.\max_{1\le k,j\le n}\left|\left\langle g_k, e_j \right\rangle\right| \tag{51}$$

Since **E** is spike matrix, **G.E=G.**
(50) can be simplified by

$$\mathbf{s} = \mathbf{G}.p(t)\big|_{t=kT} + \mathbf{n} \quad k=1\ldots N \tag{52}$$

In (52), the CS method is simplified, and the multiply complexity is reduced by MN^2. Therefore, the UWB signal is suitable for CS, moreover it makes CS simpler and reduces the computation complexity.
The recovery algorithm is

$$\arg\ \min\left\|p(t)\big|_{t=kT}\right\|_1 \text{ such that } \left\|\mathbf{G}.p(t)\big|_{t=kT} - \mathbf{s}\right\|_2 \le \varepsilon \tag{53}$$

The recovery multiply complexity is reduced by N^2.
Theorem:
Fix $p(t)\big|_{t=kT} \in \mathbb{R}^N$, and it is K sparse on a certain basis Ψ. Select M measurements in the Φ domain uniformly at random. Then if

$$M \ge c.\mu^2(\Phi,\Psi).K.\log N \tag{54}$$

For some positive constant c, the solution to (10) is success with high probability. From (54), we see that M is proportional to three factors: μ, K and N. If μ and N are fixed, the sparser K can reduce the measurements needed to reconstruct the signal. From Fig.29, we see that the spike basis can recover the signal.

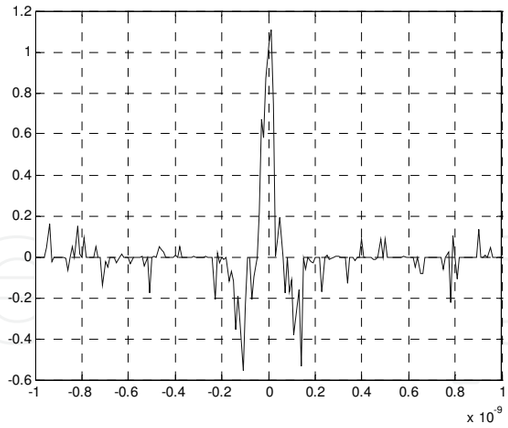

Fig. 29. Reconstructed signal from measurementsat 20% of the Nyquist rate

In this part, examples are done to show the comparison of the proposed method with traditional methods.
In all of the examples, the transmitted signal is expressed as

$$s(t) = (1 - 4\pi(\frac{t}{0.2\times 10^{-9}})^2) \times \exp(-2\pi(\frac{t}{0.2\times 10^{-9}})^2) .$$

The bandwidth of the signal is 2.5GHz, and the traditional sampling frequency is 5GHz.

A. Example 1 (in LOS environment)

In the first example, we assume that the signal is passed through Rician channel and the number of multipath is six. In the first simulation (see Fig.30), we set the observed time is 0.2um. Fig.30(a) shows the UWB signal without channel interference. Fig.30(b) shows the

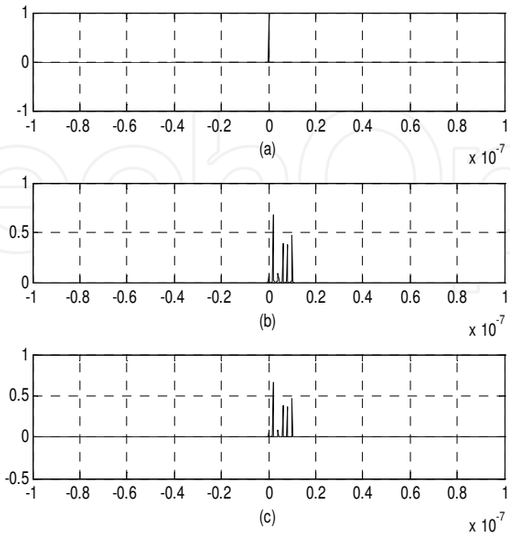

Fig. 30. (a) Ideal reconstructed UWB signal (b) Reconstructed UWB signal with Nyquist rate (c) Reconstructed UWB signal with 10% of the Nyquist rate

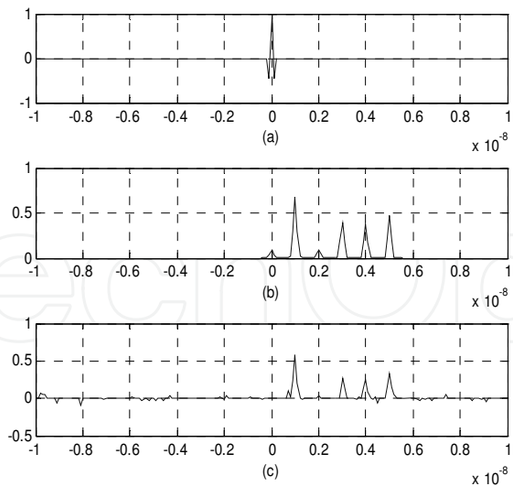

Fig. 31. (a) Ideal reconstructed UWB signal (b) Reconstructed UWB signal with Nyquist rate (c) Reconstructed UWB signal with 30% of Nyquist rate

reconstructed UWB signal at Nyquist sampling rate. Fig30(c) shows the reconstructed signal by 10% of the Nyquist sampling rate. The time delay error of both methods is about 1nm.

In the second simulation (see Fig.31), we shorten the observed time to 0.02um, all of the other parameters are the same. Fig.31(c) shows the measurement we need to reconstruct the signals is up to 30%. And much more details of the signal can be seen. And the time delay error is 1nm.

Comparing these two simulations, the conclusion is that 1) by using 10% of Nyquist sampling rate, the accuracy of TOA estimation is the same as that by using full Nyquist rate. 2) By enlarging the sampling rate by 30%, more detail information of the signal can be recovered. However, for TOA estimation, we do not need to recover the full signal but the peak location of the signal which makes the use of 10% Nyquist sampling rate possible.

B. Example 2 (in NLOS environment)

In the second example, we simulate the TOA estimation of UWB signal in NLOS environment (the number of multipath is set to six).

At the first simulation (see Fig.32), we set the observed time is 0.2um. Fig.32(a) shows the ideal received UWB signal without Rayleigh channel interference. Fig.32(b) shows the detected UWB signal at Nyquist sampling rate. Fig.32(c) shows the detected UWB signal at 11% Nyquist sampling rate by using our method. We can see that Fig.32(c) can recover the signal (in Fig.32(b)) well, although lose some detail information. And the time delay errors of them are both 1nm.

At the second simulation (see Fig.33), we shorten the observed time to 0.02um, all of the other parameters are the same. It is shown in Fig.33(c) that the measurement we need to reconstruct the signals is 35% and much more details of the signal can be seen compared with Fig.33(c). And the time delay error is 1nm.

Comparing these two simulations, the conclusion is that 1) the accuracy of TOA estimation achieved by 11% Nyquist sampling rate is the same as that by full Nyquist sampling rate. 2) When more sampling rate is used, more detail information can be recovered. However, in TOA estimation, we do not need to recover the whole signal but the peak location of the

signal. Finally, we can get the TOA estimation by 11% Nyquist sampling rate and the drawback is that some detail information of the signal is lost.

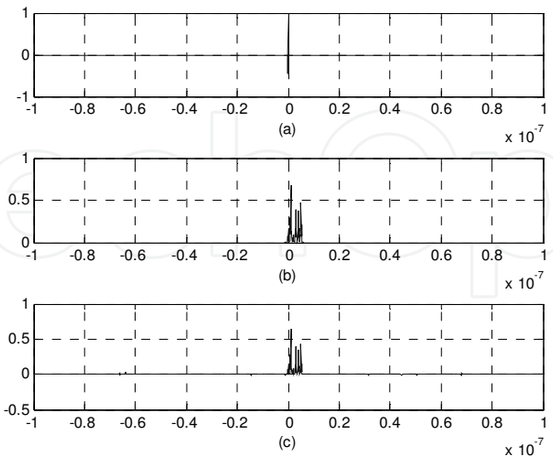

Fig. 32. (a)Ideal reconstructed UWB signal (b) Reconstructed UWB signal with Nyquist rate (c) Reconstructed UWB signal with 11% of the Nyquist rate

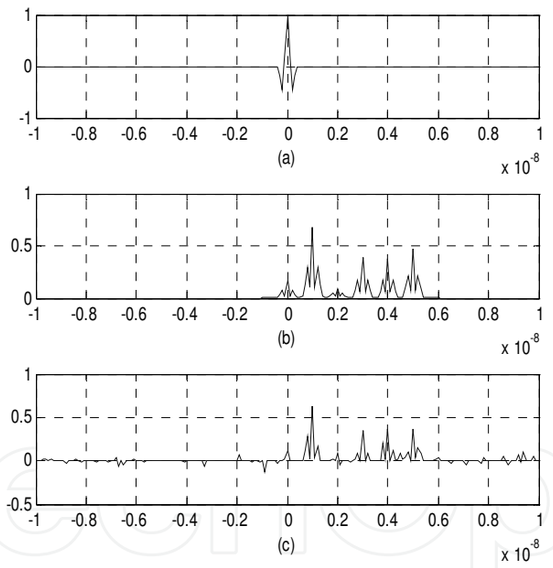

Fig. 33. (a)Ideal reconstructed UWB signal (b)Reconstructed UWB signal with Nyquist rate (c) Reconstructed UWB signal with 35% of Nyquist rate

3.3.3 Tracking system

Fig.34. is Ubisense precise real time location system, tracking unlimited number of people and objects in any space of any size with 15cm 3D tracking accuracy and high reliability. In this system, Ubisense UWB hardware is the platform and Ethernet (wire/wireless) is used as a transmission network. The UWB sensors are deployed around the room, generally on the wall. The target is attached with a UWB tag. When the target come into the area where is

covered by UWB sensors, the sensors locate the target and provide location and speed information to the user.

UWB tracking systems have inherent advantages over other technologies:

a. Exceptional performance —Performs in high multi-path environments
b. Excellent real-time location accuracy — Better than 30cm (1 foot)
c. Long tag battery life —Up to 7 years at 1 Hz blink rate
d. Long Range — Up to 200 meters (650 feet) with line of sight
e. Unmatched real-time location tag throughput — Up to2700 tags/hub
f. Fast tag transmission rates —Up to 25 times/second
g. Fast intuitive setup — typical single location set-up in one day

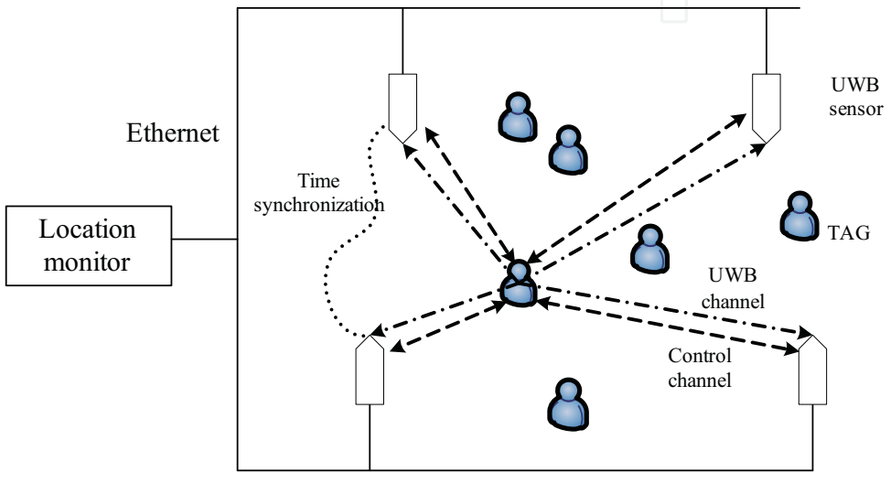

Fig. 34. UWB real time location system

3.4 Smart antennas technique

Smart antennas are often used for providing accurate AOA estimation. The commonly used methods for AOA estimation are beam forming (BF) (Van, 1998), minimum variance distortionless response (MVDR), multiple signal classification (MUSIC) (Vaidyanathan, 1995), maximum likelihood (ML) (Stoica, 1990).

3.4.1 Array signal processing

Before we describe the conventional methods of AOA estimation, it is necessary to present the array signal processing issues by smart antennas. In the array signal process, there are four issues of interest:

a. Array configuration
b. Spatial and temporal characteristics of the signal
c. Spatial and temporal characteristics of the interference
d. Objective of the array processing

Here, we consider the smart antenna as a uniform linear array (ULA). For the second issue, we set the signal structure as a known plane-wave signal from unknown directions. The interference is white Gaussian noise that is statistically independent in time and space domain. The objective is to estimate the AOA of multiple plane-wave signals in the presence of noise.

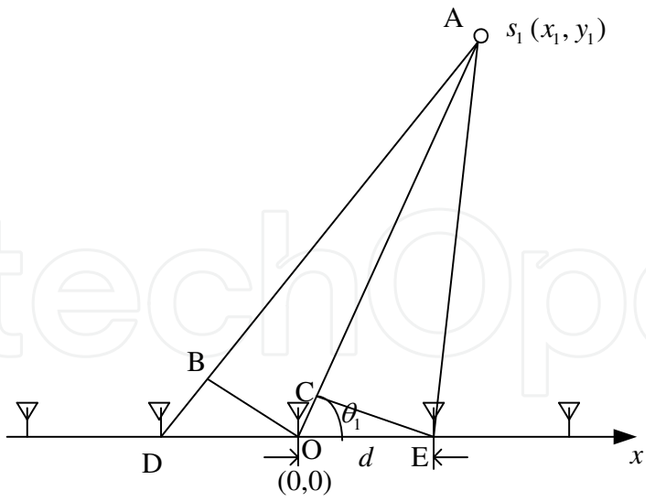

Fig. 35. Array processing observation model

3.4.2 AOA estimation methods

Before we describe the conventional methods of AOA estimation, it is necessary to present the mathematical model for the problem. Consider the basic case, the narrowband sources in the farfield of a uniform linear arrays (ULA) as shown in Fig.35. ULA consists of M omni-directional sensors with equal spacing d, residing on the x-coordinate axis. Taking the phase center of the array at the origin, the position of the m-th sensor is

$$p_m=(m\text{-}(\mathrm{M}+1)/2)d,\ m\in\{1,\ldots M\}$$

The modulated signal in narrowband case can be expressed as $u(t)\exp(j\omega_0 t)$, where $u(t)$ is the baseband signal.

The output of the sensor at origin is

$$y_0(t)=u(t-\tau_{center})\exp(j\omega_0(t-\tau_{center})) \tag{55}$$

τ_{center} is the delay from the source to the phase-center. After demodulating, it can be represented as

$$y_0(t)=u(t-\tau_{center})\exp(-j\omega_0\tau_{center}) \tag{56}$$

Assume that the time delay relative to the origin sensor is τ_m

The output of sensor m is

$$y_m(t)=u(t-\tau_{center}-\tau_m)\exp(j\omega_0(-\tau_{center}-\tau_m)) \tag{57}$$

Since the signal is narrowband, it is able to ignore the delay between the sensors.

$$y_m(t)=u(t-\tau_{center})\exp(j\omega_0(-\tau_{center}-\tau_m)) \tag{58}$$

By measuring time relative to the phase center, the dependence on τ_{center} can be dropped. Thus, the output of sensor m is

tfor a single source, the complex envelope of the sensor outputs has the following form:

$$y_m(t) = u(t)\exp(-j\omega_0\tau_m) \tag{59}$$

where $\tau_m = -\dfrac{(m-(M+1)/2)}{c} d\cos\theta_1$

$$y_m(t) = u(t)\exp(j\omega_0(\frac{(m-(M+1)/2)}{c} d\cos\theta_1)) \tag{60}$$

Define $k^T p_m = -(\omega_0 / c)(m-(M+1)/2)d\cos\theta_1$, $k = \omega_0 / c$, therefore,

$$y_m(t) = u(t)\exp(-jk^T p_m) \tag{61}$$

Define angle vector $\mathbf{a}(\theta_1) = \exp(-jk^T\mathbf{p})$

Thus, for a single source, the complex envelope of the sensor outputs has the following form:

$$\mathbf{y}(t) = \mathbf{a}(\theta_1)u(t) + \mathbf{n}(t) \tag{62}$$

Define angle matrix $A(\theta) = [\mathbf{a}(\theta_1)^T, \mathbf{a}(\theta_2)^T ..., \mathbf{a}(\theta_K)^T]$, where $\boldsymbol{\theta} = [\theta_1, ..., \theta_K]$ is the vector of unknown emitters' AOAs, The (*m*,*k*) element represents the *k*th source AOA information to the *m*th sensor. $\mathbf{u}(t) = [s_1(t), s_2(t), ..., s_k(t)]'$ is the signals from K emitters. Taking noise into account, the final version of the model takes the following form:

$$\mathbf{y}(t) = \mathbf{A}(\boldsymbol{\theta})\mathbf{u}(t) + \mathbf{n}(t) \tag{63}$$

In order to characterize the arriving signal, several time samples are required, this is the Snapshot Model

$$\mathbf{y}(t) = \mathbf{A}(\boldsymbol{\theta})\mathbf{u}(t) + \mathbf{n}(t), \quad t = 1, 2, ...N \tag{64}$$

For simplicity, the noise is assumed to be spatially and temporally stationary and white, uncorrelated with the source. The covariance matrix takes the following form:

$$\mathrm{E}[\mathbf{n}(t)\mathbf{n}^H(t)] = \sigma^2\mathbf{I}$$

Where **I** is an identity matrix.

The covariance of the baseband signal $u(t)$ is given by

$$\mathbf{P} = \mathrm{E}[\mathbf{u}(t)\mathbf{u}^H(t)] = \lim_{N\to\infty} \frac{1}{N}\sum_{t=1}^{N} \mathbf{u}(t)\mathbf{u}^H(t) \tag{65}$$

N times snapshots approximation is computed by

$$\hat{P} = \frac{1}{N}\sum_{t=1}^{N} \mathbf{u}(t)\mathbf{u}^H(t) \tag{66}$$

The covariance of the sensor output signal $y(t)$ is given by

$$\mathbf{R} = \mathrm{E}[\mathbf{y}(t)\mathbf{y}^H(t)] = \mathrm{A}(\theta)\mathrm{P}\mathrm{A}^H(\theta) + \sigma^2\mathbf{I} \tag{67}$$

N times snapshots approximation is used:

$$\hat{\mathbf{R}} = \frac{1}{N}\sum_{t=1}^{N}\mathbf{y}(t)\mathbf{y}^H(t) \tag{68}$$

A. Beamforming

The beamforming method uses complex weights $\mathbf{w}$ on the sensors output to achieve maximum power. The array output thus becomes

$$z(t) = \mathbf{w}^H\mathbf{y}(t) \tag{69}$$

$$P_{bf}(\theta) = \mathrm{E}[z(t)z^H(t)] = \mathbf{w}^H\mathrm{E}[\mathbf{y}(t)\mathbf{y}^H(t)]\mathbf{w} = \mathbf{w}^H\mathbf{R}\mathbf{w} \tag{70}$$

For simplicity, we assume that the source comes from the direction of θ_1, then the output power is given by

$$\begin{aligned} P &= \mathrm{E}[\mathbf{w}^H\mathbf{y}(t)\mathbf{y}^H(t)\mathbf{w}] = \mathbf{w}^H\mathrm{E}[\mathbf{y}(t)\mathbf{y}^H(t)]\mathbf{w} \\ &= \mathbf{w}^H\mathrm{E}[(\mathbf{a}(\theta_1)u_1(t) + \mathbf{n}(t))(u_1(t)^H\mathbf{a}^H(\theta_1) + \mathbf{n}^H(t))]\mathbf{w} \\ &= \mathbf{w}^H[\mathbf{a}(\theta_1)\mathrm{E}[u_1(t)u_1(t)^H]\mathbf{a}^H(\theta_1) + \sigma^2\mathbf{I}]\mathbf{w} \\ &= \mathbf{w}^H\mathbf{a}(\theta_1)\mathrm{E}[u_1(t)u_1(t)^H]\mathbf{a}^H(\theta_1)\mathbf{w} + \mathbf{w}^H\sigma^2\mathbf{I}\mathbf{w} \\ &= \left\|\mathbf{w}^H\mathbf{a}(\theta_1)\right\|_2^2\mathrm{E}[u_1(t)u_1(t)^H] + \mathbf{w}^H\mathbf{w}\sigma^2\mathbf{I} \end{aligned} \tag{71}$$

From the above equation, it is observed that when $\mathbf{w} = \mathbf{a}(\theta_1)$, the power is maximum. From the view of physical concept, the maximum power is achieved by steering at the direction from which the waves are arriving.
The normalized form of $\mathbf{w}$ is given by

$$\mathbf{w} = \frac{\mathbf{a}(\theta)}{\left\|\mathbf{a}(\theta)\right\|} \tag{72}$$

Thus, the output power takes the form:

$$P_{bf}(\theta) = \frac{\mathbf{a}^H(\theta)\mathbf{R}\mathbf{a}(\theta)}{\left\|\mathbf{a}(\theta)\right\|^2} \tag{73}$$

In practice, the N times snapshots are used to compute the power

$$\hat{P}_{bf}(\theta) = \frac{\mathbf{a}^H(\theta)\hat{\mathbf{R}}\mathbf{a}(\theta)}{\left\|\mathbf{a}(\theta)\right\|^2} \tag{74}$$

Where $\hat{\mathbf{R}} = \frac{1}{N}\sum_{t=1}^{N}\mathbf{y}(t)\mathbf{y}^H(t)$

Beamforming is a very simple and robust approach, which is widely used in practice. However, the method performance cannot be improved by increasing SNR or observation time.

B. Minimum variance distortionless response (MVDR)

The classical beamforming method has weights which are independent of the signals and noise.

The idea of MVDR is to use the estimated signal and noise parameters to improve the performance. It attempts to minimize the variance due to noise, while keeping the gain in the direction of steering equal to unity:

$$\mathbf{w}(\theta) = \arg\min_w(\mathbf{w}^H\mathbf{R}\mathbf{w}),\ \text{subject to}\ \mathbf{w}^H\mathbf{a}(\theta) = 1$$

The solution of this optimization problem can be shown to have the following form:

$$\mathbf{w} = \frac{\mathbf{R}^{-1}\mathbf{a}(\theta)}{\mathbf{a}^H(\theta)\mathbf{R}^{-1}\mathbf{a}(\theta)} \tag{75}$$

The resulting spectrum has an expression as:

$$P(\theta) = \mathbf{w}_{opt}\mathbf{R}\mathbf{w}_{opt} = \frac{\mathbf{a}^H(\theta)\mathbf{R}^{-1}\mathbf{R}\mathbf{R}^{-1}\mathbf{a}(\theta)}{[\mathbf{a}^H(\theta)\mathbf{R}^{-1}\mathbf{a}(\theta)]^2} = \frac{1}{\mathbf{a}^H(\theta)\mathbf{R}^{-1}\mathbf{a}(\theta)} \tag{76}$$

The main benefit of this method is a substantial increase in resolution compared with beamforming. The resolution increases without limit as SNR or the observation time are increased. Shortcomings include an increase in the amount of computation compared to beamforming, poor performance with small amounts of time-samples and inability to handle strongly correlated or coherent sources.

C. Multiple signal classification (MUSIC)

The MUSIC method is the most prominent member of the family of eigen-expansion based source location estimators. The underlying idea is to separate the eigenspace of the covariance matrix of sensor outputs into the signal and noise components using the knowledge about the covariance of the noise. The sensor output correlation matrix admits the following decomposition:

$$\mathbf{R} = \mathrm{A}(\theta)\mathrm{P}\mathrm{A}^H(\theta) + \sigma^2\mathbf{I} = \mathbf{U}\mathbf{\Lambda}\mathbf{U}^H = \mathbf{U}_s\mathbf{\Lambda}_s\mathbf{U}_s{}^H + \mathbf{U}_n\mathbf{\Lambda}_n\mathbf{U}_n{}^H \tag{77}$$

$\mathbf{U}$ and $\mathbf{\Lambda}$ form the eigenvalue decomposition of $\mathbf{R}$, and $\mathbf{U}_s, \mathbf{\Lambda}_s$ are the partitions of signal subspace, $\mathbf{U}_n, \mathbf{\Lambda}_n$ are the partitions of noise subspace, $\mathbf{\Lambda}_n$ equals to σ^2。Provided that $\mathrm{A}(\theta)\mathrm{P}\mathrm{A}^H(\theta)$ has rank *K*. The number of sources, *K* has to be strictly less than the number of sensors *M*. $\mathbf{R}$ has *K* eigenvalues which are due to the combined signal plus noise subspace, and *M-K* eigenvalues due to the noise subspace. Due to the orthogonality of eigensubspaces corresponding to different eigenvalues for Hermitian matrices, the noise subspace is orthogonal to the direction vector of signals, thus

$$\mathbf{U}_n^H\mathbf{a}(\theta) = 0 \tag{78}$$

MUSIC spectrum is obtained by putting the squared norm of this term into the denominator, which leads to very sharp estimates of the positions of the sources

$$P_{MUS}(\theta) = \frac{1}{\mathbf{a}^H(\theta)\mathbf{U}_n\mathbf{U}_n^H\mathbf{a}(\theta)} \tag{79}$$

In contrast with the previously discussed techniques, MUSIC spectrum has no direct relation to power, also it cannot be used as a beamformer, since the spectrum is not obtained by steering the array. MUSIC provides a consistent estimate of the locations of the sources, as SNR and the number of sensors go to infinity. Despite the dramatic improvement in resolution, MUSIC suffers from a high sensitivity to model errors, such as sensor position uncertainty. Also, the resolution capabilities decrease when the signals are correlated. When some of the signals are coherent, the method fails to work. The computational complexity is dominated by the computation of the eigenexpansion of the covariance matrix.

D. Sparsity angle sensing (SAS)

Many algorithm design challenges arise when the sources are close, Signal to Noise Ratio is low, correlated and coherent sources, less number of time samples. To improve the estimation performance and robustness, sparsity-based signal processing techniques for AOA estimation have been popularity.

To cast this problem into a sparse representation problem, the basic steps are:

1. Construct a known vector $\tilde{\boldsymbol{\theta}}$ which is the expansion of vector $\boldsymbol{\theta}$ considering all possible source locations. Let $\tilde{\boldsymbol{\theta}}$ be filled with N vectors $\{\theta_1,...,\theta_N\}$ which are the possible locations of unknown emitters. $\Delta(\tilde{\theta})$ is the ideal spatial resolution ability.
2. Fill each column of $\tilde{\mathbf{A}}(\tilde{\theta})$ with each potential emitter location: $\tilde{\mathbf{A}} = [\mathbf{a}(\tilde{\theta}_1), \mathbf{a}(\tilde{\theta}_2), ..., \mathbf{a}(\tilde{\theta}_N)]$. Suppose the number of sensor arrays is M, the number of all possible emitters is N, the number of real unknown emitters is K. $\tilde{\mathbf{A}}$ is a $M \times N$ matrix. The relationship among M, N and K is $K<M<N$.
3. Reconstruct the output signal model as

$$\mathbf{y}(t) = \hat{\mathbf{A}}(\boldsymbol{\theta})\hat{\mathbf{u}}(t) + \mathbf{n}(t)$$

   Where $\hat{\mathbf{u}}(t) = [u_1(t), u_2(t), ...u_N(t)]$ represents a N virtual transmitted signal vector in which only the signal corresponding to the true angle directions are non-zero, other directional signals are zero, which means $\|\hat{\mathbf{u}}(t)\|_0 = K$
4. The nonzero elements of $\hat{\mathbf{u}}(t) = [u_1(t), u_2(t), ...u_N(t)]$ corresponds to the estimated AOAs. Thus, the AOA estimation could be transfered to the estimation o $\hat{\mathbf{u}}(t)$. First to solve $\hat{\mathbf{u}}(t)$ and then get the AOAs.
5. $\hat{\mathbf{u}}(t)$ can be solved by l_1-denoise optimization algorithm with quadratic constraints.

$$\min \|\hat{\mathbf{u}}(t)\|_1 \quad \text{subject to} \quad \left\|\mathbf{y}(t) - \hat{\mathbf{A}}(\boldsymbol{\theta})\hat{\mathbf{u}}(t)\right\|_2 \le \varepsilon \tag{80}$$

   where $\|\hat{\mathbf{u}}(t)\|_1 = \sum_{i=1}^{K} |u_i(t)|$, ε is the error threshold.

Several experimental results are shown by comparing four AOA estimation approaches: BF, MVDR, MUSIC and SAS.

In Fig.36., the SNR is -7dB and the distance between two sources are 20°, all the methods are able to solve the two sources. In Fig.37., the SNR is still -7dB, but the distance between two sources are close to 10° separation, the BF method begins to merge the two peaks while the other three methods are able to solve two sources. In Fig.38., when the two sources are close to 4° separation, SNR is -1dB, BF, MVDR and MUSIC all emerge except SAS. Four approaches are compared and the results demonstrate that SAS outperforms the other three approaches in terms of robustness and spatial resolution.

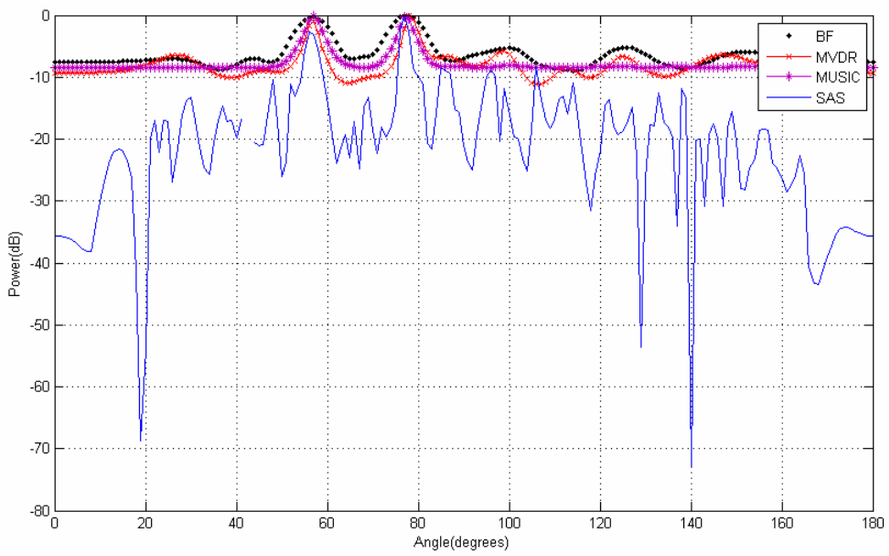

Fig. 36. Spatial spectra for BF, MVDR, MUSIC and SAS. SOAs: 57°and 77°.SNR=-7dB

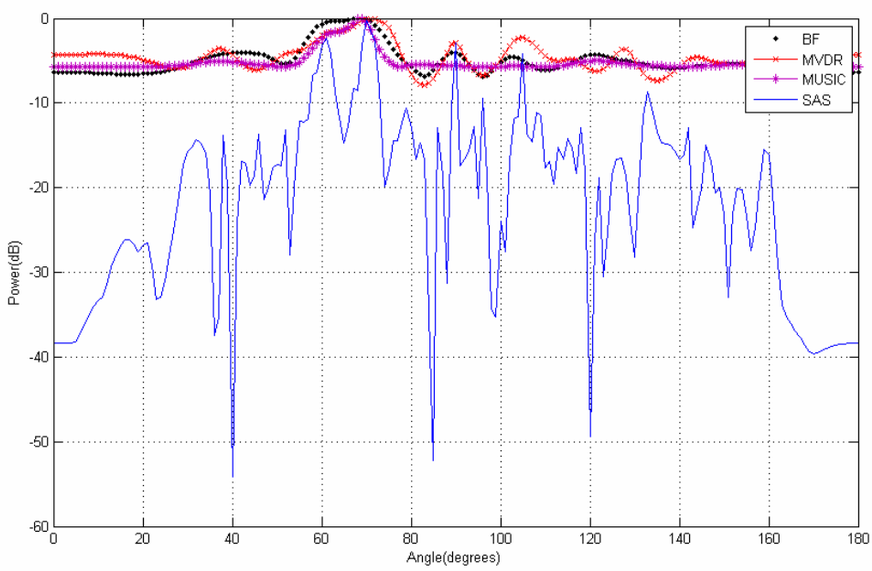

Fig. 37. Spatial spectra for BF, MVDR, MUSIC and SAS. AOAs: 60°and 70°.SNR=-7dB

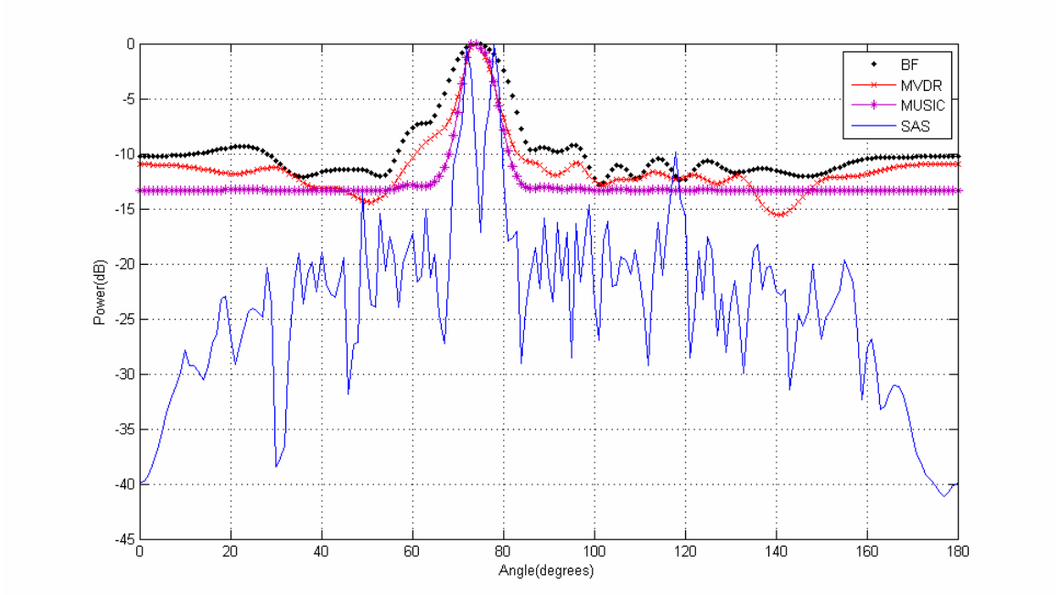

Fig. 38. Spatial spectra for BF, MVDR, MUSIC and SAS. AOAs: 73°and 77°,SNR=-1dB

4. Conclusion

This chapter is focused on the design and analysis of wireless positioning systems. An overview of basic principles, latest developed systems and state of the art signal processing techniques for wireless positioning are presented. This chapter aims to provide the concepts related to localization systems as well as the methods to localize terminals in different wireless networks. As an important part of the chapter, potential challenges and new techniques for wireless positioning are provided to the readers. The authors hope that this chapter will help readers identify the key technical challenges in wireless positioning and be interested in this emerging area.

5. Acknowledgement

This work was supported by Campus Talent Grant No. W10RC00040, the National Science and Technology Major Project Grant No.2009ZX03003-008-02 and National Science Foundation No.61071075.

6. References

Alavi, B. & Pahlavan, K. (2006). Modeling of the TOA-based distance measurement error using UWB indoor radio measurements. *Communications Letters, IEEE*, Vol.10, No.4, pp.275-277, ISSN 1089-7798

Barabell A.J. (1983). Improving the resolution performance of eigenstructure based direction-finding algorithms. *IEEE international conference on acoustics, speech, and signal processing*, pp. 336-339

Candès, E. J. & Wakin, M. B. (2008). An introduction to compressive sampling. *IEEE Signal Processing Magazine*, Vol.25, No.2, pp. 21-30

Catovic, A.Sahinoglu, Z. (2004). The Cramer-Rao bounds of hybrid TOA/RSS and TDOA/RSS location estimation schemes. *Communications Letters, IEEE*, Vol.8, No.10, pp.626-628, ISSN 1089-7798

Chan Y.T.& Ho K.C. (1994). A simple and efficient estimator for hyperbolic location. *IEEE Trans on Signal Processing*, Vol. 42, No.8, pp. 1905-1915

Cong, L. & Weihua Z. (2001). Non-line-of-sight error mitigation in TDOA mobile location. *GLOBECOM '01. IEEE* , Vol.1, No.pp.680-684

Candès, E. J.; Romberg J.& Tao T. (2006). Robust uncertainty principles: Exact signal reconstruction from highly incomplete frequency information. *IEEE Trans. Inform. Theory*, Vol.2,No.2, pp.489-509

Fang B.T. (1990). Simple solutions for hyperbolic and related position fixes. *IEEE Trans on AES*, Vol. 26, No.9, pp.748-753

Friedlander B. (1987). A passive localization algorithm and its accuracy analysis. *IEEE J. Ocean. Eng.*, Vol.12, No.1, pp. 234-245

Foy W. H., (1976) Position-location solutions by Taylor-series estimation . *IEEE Trans on AES*, Vol.12, No.3, pp. 187-194

Gezici, S. et al. (2005). Localization via ultra-wideband radios: a look at positioning aspects for future sensor networks. *Signal Processing Magazine, IEEE*, Vol.22, No.4, pp.70-84, ISSN 1053-5888

Gershman, A.B. (2003).Robust adaptive beamforming: an overview of recent trends and advances in the field. *International Conference on Antenna Theory and Techniques*, pp.30-35, Sevastopol, Ukraine

Guolin, S. (2005). Signal processing techniques in network-aided positioning: a survey of state-of-the-art positioning designs. *Signal Processing Magazine, IEEE*, Vol.22, No.4, pp.12-23, ISSN 1053-5888

Jian Z.; Durgin, G.D. (2005). Indoor/outdoor location of cellular handsets based on received signal strength. *Vehicular Technology Conference*, Vol. 1, pp. 92 - 96

Kleine-Ostmann T. & Bell A.E. (2001). A data fusion architecture for enhanced position estimation in wireless networks. *IEEE Communications Letters*, Vol.5, No.8, pp. 343-345

Porretta, M. et al. (2004). A novel single base station location technique for microcellular wireless networks: description and validation by a deterministic propagation model. Vehicular Technology, *IEEE Transactions on*, Vol. 53, No.5, pp. 1502-1514, ISSN 0018-9545

Pahlavan, K.; Xinrong, Li & Makela, J. P. (2002). Indoor geolocation science and technology. *Communications Magazine, IEEE*, Vol.40, No.2, pp. 112-118, ISSN 0163-6804

Porcino, D. & Hirt, W. (2003). Ultra-wideband radio technology: potential and challenges ahead. *Communications Magazine, IEEE*, Vol.41, No., pp.66-74, ISSN 0163-6804

Rappaport, T.S.; Reed J.H. (1996). Position Location Using Wireless Communications on Highways of the Future. *IEEE Communications Magazine*, Vol.34, No.10, pp.33-41

Reed, J. H. et al. (1998). An overview of the challenges and progress in meeting the E-911 requirement for location service. *Communications Magazine, IEEE*, Vol.36, No.4, pp.30-37, ISSN0163-6804

Rieken, D. W. & Fuhrmann, D. R. (2004). Generalizing MUSIC and MVDR for multiple noncoherent arrays. *Signal Processing, IEEE Transactions on*, Vol. 52, No. 9, pp. 2396-2406, ISSN 1053-587X

Roy S., et al. (2004). Ultrawideband radio design: the promise of high-speed, short-range wireless connectivity. Proceedings of the IEEE, Vol.92, No. 2, pp. 295-311

Richard B. (2007). Compressive sensing. *IEEE Signal Processing Magzine*, Vol.24, No.4, pp.118-121.

Raleigh G. & Boros T. (1998). Joint space-time parameter estimation for wireless communication channels. *IEEE trans. on signal processing*, Vol. 46, pp.1333-1343

Stoica, Z. Wang, J. (2003). Robust capon beamforming. *IEEE Signal Processing Letters*, Vol.10, June 2003

Swindlehurst, A. Kailath, T. (1992).A performance analysis of subspace-based methods in the presence of model Errors-Part 1: the MUSIC algorithm. *IEEE Trans. Signal Processing*, Vol.40, No.7,pp.1758-1774,July

Sayed, A. H.; Tarighat, A.& Khajehnouri, N. (2005). Network-based wireless location: challenges faced in developing techniques for accurate wireless location information. *Signal Processing Magazine, IEEE*, Vol.22, No.4, pp.24-40, ISSN1053-5888

Thomas N.; Cruickshank D. & Laurenson D. (2001). Performance of a TDOA/AOA hybrid mobile location system. *International conference on 3G mobile communication technologies,* pp. 216-220

Vaughan-Nichols, S. J.(2009). Will Mobile Computing's Future Be Location, Location, Location? *IEEE Computer*,Vol.42, No.2, pp. 14-17, ISSN 0018-9162

Vanderveen M.; Papadias C. & Paulraj A. (1997). Joint angle and delay estimation for multipath signals arriving at an antenna array. *IEEE communication letters*, Vol. 1, pp. 12-14

Van, B.D. & Buckley, K.M. (1998). Beamforming: a versatile approach to spatial filtering. *IEEE ASSP Magzine*, Vol.5, pp.4-24

Vaidyanathan C.& Buckley, K.M. (1995). Comparative studies of MUSIC and MVDR location estimators for model perturbations. *IEEE International Conference on Acoustics, Speech and Signal Processing*, Vol.3, pp.9-12,1995

Wax M.; Leshem A. (1997). Joint estimation of time delays and directions of arrival of multiple relections of a known signal. *IEEE trans. on signal processing*, Vol. 45, PP.2477-2484

Wylie, M.P. & Holtzman, J. (1996). The non-line of sight problem in mobile location estimation. *5th IEEE International Conference on Universal Personal Communications*, Vol.2, No.29, pp. 827-831

Zagami, J. M. (1998). Providing universal location services using a wireless E911 location network. *Communications Magazine, IEEE*, Vol.36, No.4, pp. 66-71, ISSN 0163-6804

Zhao, L.; Yao, G.&Mark, J.W. (2006). Mobile positioning based on relaying capability of mobile stations in hybrid wireless networks. *IEE Proceedings on Communications*, Vol. 153, No.5, pp.762-770

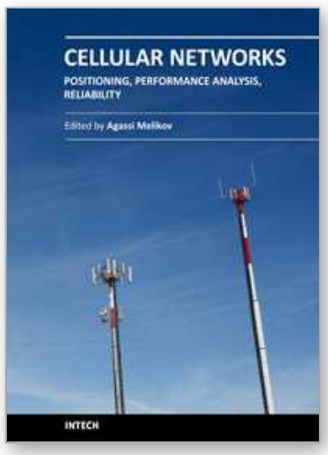

Cellular Networks - Positioning, Performance Analysis, Reliability
Edited by Dr. Agassi Melikov

ISBN 978-953-307-246-3
Hard cover, 404 pages
Publisher InTech
Published online 26, April, 2011
Published in print edition April, 2011

Wireless cellular networks are an integral part of modern telecommunication systems. Today it is hard to imagine our life without the use of such networks. Nevertheless, the development, implementation and operation of these networks require engineers and scientists to address a number of interrelated problems. Among them are the problem of choosing the proper geometric shape and dimensions of cells based on geographical location, finding the optimal location of cell base station, selection the scheme dividing the total net bandwidth between its cells, organization of the handover of a call between cells, information security and network reliability, and many others. The book focuses on three types of problems from the above list - Positioning, Performance Analysis and Reliability. It contains three sections. The Section 1 is devoted to problems of Positioning and contains five chapters. The Section 2 contains eight Chapters which are devoted to quality of service (QoS) metrics analysis of wireless cellular networks. The Section 3 contains two Chapters and deal with reliability issues of wireless cellular networks. The book will be useful to researches in academia and industry and also to post-gradute students in telecommunication specialitiies.

INTECH
open science | open minds

InTech Europe
University Campus STeP Ri
Slavka Krautzeka 83/A
51000 Rijeka, Croatia
Phone: +385 (51) 770 447
Fax: +385 (51) 686 166
www.intechopen.com

InTech China
Unit 405, Office Block, Hotel Equatorial Shanghai
No.65, Yan An Road (West), Shanghai, 200040, China
中国上海市延安西路65号上海国际贵都大饭店办公楼405单元
Phone: +86-21-62489820
Fax: +86-21-62489821

IntechOpen